Mesoscale Convective Systems in the Congo Basin: Seasonality, Regionality, and Diurnal Cycles

Patrick C. Andrews, Kerry H. Cook, Edward K. Vizy

Department of Geological Sciences
The University of Texas at Austin
Austin TX
USA

Published in *Climate Dynamics*

August 30, 2023

This preprint has not undergone any post-submission improvements or corrections. The Version of Record of this article is published in Climate Dynamics, and is available online at https://doi.org/10.1007/s00382-023-06903-7

The citation for this work is as follows:
Andrews, P.C., K.H. Cook, and E.K. Vizy 2024: Mesoscale convective systems in the Congo Basin: Seasonality, regionality, and diurnal cycles. *Clim. Dyn*., 62, 609-630. https://doi.org/10.1007/s00382-023-06903-7

Corresponding Author: Patrick C. Andrews (patrickandrews@utexas.edu)

Abstract

Twenty years of IMERG precipitation estimates are used to evaluate the contributions of mesoscale convective system (MCS) rainfall to total rainfall in the Congo Basin. Studying these systems advances our basic understanding of Congo Basin rainfall on all time scales.

The seasonality of MCS rainfall in the Congo Basin follows the seasonality of total rainfall with high rainfall in spring, summer, and fall and a winter dry season in each hemisphere. In the equinoctial seasons, MCS rainfall accounts for ≥80% of total rainfall within 5° of the equator with the highest rainfall rates occurring along the eastern and western boundaries of the basin. In boreal summer, MCS rainfall maxima occur near the Cameroon Highlands (9°E-18°E) and in boreal winter, they occur along the eastern orography (22°E-28°E). The 80% percent contribution is sustained in the continental interior (15°E-25°E, 5°S-5°N) throughout the year.

The diurnal cycle of MCS rainfall is similar to that of total rainfall. Diurnal cycles are unimodal in the equinoctial seasons but are regionally and seasonally inhomogeneous in the solstitial seasons. Regardless of modality, MCS rainfall is highest at 15Z (1600/1700 LT) and lowest at 10Z. MCS percent contribution changes little throughout the diurnal cycle but is highest (≥90%) at 04Z close to the continental interior. Larger MCSs contribute their greatest percentage of MCS rainfall (83-92%) between 04Z and 07Z, while more-intensely precipitating MCSs have no seasonally or regionally consistent diurnal cycle.

Seasonal and diurnal MCS rainfall maxima are associated with unstable MSE profiles in the lower troposphere. Changes in moisture drive the seasonal cycle of MSE while changes in temperature drive its diurnal cycle.

Key words: Congo Basin rainfall, equatorial African precipitation, African rainfall seasonality, African rainfall diurnal cycle, mesoscale convective system, IMERG

DECLARATIONS

Funding: The research was supported by the U.S. National Science Foundation Award #26-1016-20

Conflicts of Interest/Competing Interests: none

Availability of data and material: IMERG data is freely available at https://gpm.nasa.gov/data/imerg

Code availability: Figures for the analysis were produced using the GRaDs software freely available at http://cola.gmu.edu/grads/gadoc/gadoc.php, and using Python software freely available at https://www.python.org/

Authors' contributions. All three authors contributed to the final manuscript, and an MCS identification algorithm was provided by Edward Vizy.

1. *Introduction*

The Congo Basin is one of the most convectively-active areas on the planet. It contains six of the top ten and over half of the top 500 locations of highest lightning frequency within the Tropical Rainfall Measuring Mission (TRMM) satellite range (Albrecht et al. 2016) and has the largest fraction of the top 0.1% most extreme values in brightness temperature, lightning flashes per minute, and maximum height of 40-dBZ radar reflectivity (Zipser et al. 2006). The extreme nature of Congo convective proxies suggests this region is prone to intense rainfall as precipitation ice-water content and lightning flash-rate density correlate positively with instantaneous rain rates, although how they correlate to total surface rainfall is less well-understood (Petersen and Rutledge 2001, Zipser et al. 2006).

Mesoscale convective systems (MCSs) are organized systems of convective cells capable of producing heavy rain and damaging winds and that exhibit a distinct life-cycle of growth, maturity, and decay when compared to individual convective cells (Leary and Houze 1979, Zipser et al. 1982). Using the TRMM Precipitation Radar, MCSs were found to be the primary contributor of Congo Basin rainfall, delivering upwards of 70% of annual precipitation to this region (Nesbitt et al. 2005). This suggests MCSs are vital to the delivery of rainfall in the Congo Basin and play an important role in establishing the diurnal cycle of rainfall. Prior MCS studies for the Congo Basin have primarily focused on the equinoctial rainy seasons (Laing et al. 2011, Hartman et al. 2020), however, the month of maximum lightning flash rate density can occur outside the equinoctial seasons depending on the region of the Congo (Albrecht et al. 2016). An assessment of MCSs and their diurnal cycles in all four seasons is needed to further develop our understanding of rainfall delivery systems for the Congo Basin and to fully account for regional differences in MCS activity. Here we construct a 20-year climatology of MCS rainfall in the Congo Basin using Integrated Multi-satellite Retrievals for GPM (IMERG) precipitation estimates and describe its seasonal, diurnal, and regional variations. In addition, MCS contributions to total rainfall are quantified.

Background on MCS rainfall and its variability over central equatorial Africa is reviewed in Section 2. Data and methodology, including MCS identification criteria, are provided in Section 3.

Results in section 4 are in two sections: equinoctial and solstitial seasons. Connections to physical mechanisms are shown in section 5. Section 6 provides a summary and conclusions.

2. Background

MCSs are associated with high rainfall events such as flash floods and contribute a large percentage of total rainfall in the tropics and subtropics. Using data from the Tropical Rainfall Measurement Mission (TRMM), Nesbitt et al. (2005) found that 50-90% of tropical and subtropical rainfall is contributed by MCSs. Other studies with a focus on Africa confirm this result. For example, Vizy and Cook (2018) found that MCSs generated in a convective-permitting WRF model contribute over 90% of nocturnal rainfall in August over the southwestern Sahel. Similarly, Liu et al. (2019) found that MCSs identified in TRMM contributed 80% of total rainfall to sub-Saharan Africa during boreal summer. A subset of MCSs, termed mesoscale convective complexes (MCCs), strongly influence certain regions of Africa such as the northern Sahel, which received 36% of its total July rainfall from only 7 MCCs in 1987 (Laing et al. 1998). These large storm systems persist on average for 11 hours and typically form cloud shields 300,000 km^2 in size (Laing and Fritsch 1993).

Compared to sub-Saharan Africa, MCSs in the Congo Basin are less well-documented and their regional importance is unclear. Hartman et al. (2020) found that the region between 0° and 5°S shows the greatest seasonal consistency in average MCS speed and duration, but how MCSs were related to total rainfall was not quantified. Studies agree that MCSs are most abundantly generated to the west of the high terrain of the Great Rift Valley and near the Cameroon Highlands (Jackson et al. 2009, Laing et al. 2011, Hartman et al. 2020) although Vemado and Filho (2021) found that westward-propagating MCSs may initiate in East Africa and regenerate along the orography of the Rift Valley, impacting the Congo. Studies also agree that MCSs are most frequent in the afternoon between 15Z and 18Z in equatorial Africa (Jackson et al. 2009, Laing et al. 2011, Hartman et al. 2020) but achieve their largest areal extent at night as the storms mature (Nesbitt and Zipser, 2003).

The seasonal rainfall regime in the Congo Basin is often described as bimodal but this is an artifact of a large averaging region that extends over the equator (Cook and Vizy, 2022). Except for a thin strip along the equator classified as humid and several small bimodal regions in the east, Hermann and Mohr (2011) find rainfall is unimodal in Congo Basin at the seasonal scale. In the past, precipitation seasonality in the Congo has been erroneously attributed to the migration of the Intertropical Convergence Zone (ITCZ) across the basin but seasonal influences on rainfall are more complex and vary regionally. In a study examining the seasonal influence of various sea surface temperature (SST) anomalies on five sub-divisions of the Congo, Balas et al. (2007) found that rainfall in each region was affected by a unique combination of seasonal SSTs. For the Congo, Dyer et al. (2017) found that while the Indian Ocean and local evapotranspiration are the primary sources of precipitable moisture for the Congo, their relative importance may shift as contributions from other sources of moisture such as the Atlantic shift seasonally.

Observational studies of Congo precipitation are largely satellite-based as only a handful of rain gauge stations remain operational (Nicholson et al. 2018). Without calibration from ground measurements, satellite rainfall estimates can differ by up to 2000 mm per year between datasets (Washington et al. 2013) and blended satellite and gauge datasets can produce spurious trends if the quantity of rain gauges decreases over the study period (Maidment et al. 2015). Such a decrease has happened over the last century in the Congo. However, satellite-based observation continues to improve through advances in sensor technology and international collaboration such as with the deployment of the Global Precipitation Measurement mission (GPM) and its core observatory.

In this paper, we present a climatological assessment of MCSs (2000-2020) with a regional emphasis. We examine how MCS rainfall varies over the seasonal and diurnal cycles and consider how those cycles may change regionally. We do not seek to diagnose variability in MCS storm morphology or rainfall mechanisms but this paper provides a valuable foundation for future diagnostic research.

3. Data and Methodology

3.1 Data

Precipitation estimates from the IMERG gridded precipitation dataset for 2000-2020 (Huffman et al. 2019) are analyzed in this paper. The 0.1°-resolution IMERG final run product 3BIMERGHHR merges microwave and microwave-calibrated infrared estimates from numerous satellites, providing rainfall estimates every 30 minutes. For years prior to 2014, IMERG V06 recalibrates estimates initially calibrated to TRMM to GPM in order to extend the IMERG dataset back to 2000 and to produce a consistent temporal and spatial resolution. V06 improvements to grid point interpolation and satellite intercalibration have improved IMERG's ability to capture the diurnal cycle compared to similar observational datasets (Tan et al. 2019). IMERG also validates well at the synoptic scale over Africa (Dezfuli et al. 2017) and its predecessor TRMM Multi-satellite Precipitation Analysis (TMPA) demonstrates excellent agreement with rain gauges in West Africa on monthly timescales (Nicholson et al. 2003). IMERG is chosen here for estimating MCS rainfall over the rain-gauge sparse Congo Basin for its high spatial and temporal resolutions, including its ability to capture the diurnal cycle of rainfall.

The Congo Basin is defined here as western equatorial Africa between 10°S-10°N and 9°E-30°E. This area is further sub-divided by latitude into four 5° averaging regions which extend from the Atlantic coast to 30°E (Fig. 1). Box 1 spans 10°N – 5°N, box 2 from 5°N to 0°, box 3 from 0° to 5°S, and box 4 from 5°S to 10°S. Averaging regions are determined from areas of coherent MCS contribution to total rainfall in Figures 3 and 8 as well as from areas of similar diurnal and seasonal peak rainfall via a grid point analysis (not shown).. Elevations exceeding 1000m occur in boxes 1 and 4, and near the eastern boundaries of boxes 2 and 3. The interiors of boxes 2 and 3 are at lower elevations (≤400m) than their surroundings and elevations exceeding 600m divide the interiors of boxes 2 and 3 from the Atlantic coast. Rainfall in this region progresses northward across the Congo from austral summer to boreal summer, with peaks most often concentrated near high terrain (Fig 1a-d).

3.2 Methodology

Rainfall rate thresholds and size criteria are used to identify MCSs, similar to previous studies (Laurent et al. 1998, Laing et al. 1998, Durkee et al. 2009, Laing et al. 2011, Hartman et al. 2020). Individual MCS storms are not tracked in this study, but rather, MCS rainfall is identified every half-hour for the 20-year period. We define MCS rainfall as a rainfall rate of 25 mm day^{-1} or greater that occupies at least 2000 km^2 area. These criteria are consistent with past studies (Vizy and Cook 2019, Vizy and Cook 2018, Liu et al. 2019). While the 25 mm day^{-1} rain rate may exclude some smaller MCS rainfall rates associated with the stratiform rain anvil and decay of the cloud shield (Roca et al. 2017), the threshold must be high enough in order to isolate MCS rainfall from weaker convective events over the 20-year period. As such, results presented in this paper may slightly underestimate MCS rainfall. A 2000 km^2 rain-shield threshold is commonly used in MCS studies (Mohr and Zipser 1996, Nesbitt and Zipser 2003, Vizy and Cook 2019, Liu et al. 2019) to distinguish more disorganized convective activity from organized systems of thunderstorms. Roca et al. (2017) found that 97% of tropical MCSs attained sizes larger than 5000 km^2 which suggests our size threshold selection should not impact results.

Since there may be some dependency of the results on the selection of these threshold values, additional thresholds at higher values are applied and compared to our results to test the sensitivity of threshold choice. This includes using an increased rain rate threshold of 100 mm day^{-1} over a contiguous area of 2000 km^2 (abbreviated throughout the paper as **LRR MCS**) and a larger size threshold of 10,000 km^2 that rain contiguously at least 25 mm day^{-1} (**LS MCS**). The choice of higher threshold values is somewhat arbitrary, however, the values are selected to be large enough to contrast the lower threshold MCS rainfall but not so large as to be infrequent.

After MCS rainfall has been identified, it is compared with the MCS percent contribution to total rainfall (MCS rainfall divided by total rainfall) in order to evaluate the importance of MCS rainfall to total rainfall. The use of both metrics allows us to identify when high MCS rainfall has a low percentage contribution to total rainfall or vice versa.

Additionally, MCS percent contribution at the higher thresholds is used to examine how MCS characteristics such as areal size and rainfall intensity vary throughout the diurnal cycle. This provides information on whether peaks in the diurnal cycle occur because of an increase in MCS size, an increase in MCS rainfall intensity, or a combination of both. Peaks may also occur due to changes in the number of MCSs, however, we do not count MCSs in this study. We choose not to count storms because we do not track individual storms through space or time due to the dynamic behavior and life cycle of storms. Because of this, an MCS count metric would be flawed. However, a peak associated with neither larger nor more intensely raining MCSs may by elimination be associated with an increase in the number of

MCSs. Note that MCS percent contribution for the higher thresholds is calculated by dividing the higher threshold MCS rainfall by the lower threshold MCS rainfall, not by total rainfall. This is because the LS and LRR MCS rainfall are already included within "total" MCS rainfall identified at the lower thresholds.

To assess MCS modality over the diurnal cycle, several quantitative criteria are applied to MCS rainfall, similar to prior studies (Zhang et al. 2016, Liu et al. 2019). Diurnal cycles are calculated as the mean rainfall rate that occurs at each half-hour interval. A *peak* is defined as when MCS rainfall is at least 0.5 mm day^{-1} higher than MCS rainfall ±3 hours away. The threshold value of 0.5 mm day^{-1} was selected as it successfully distinguishes between the sharp and gentle decreases in MCS rainfall in the diurnal cycle shown in Figures 4 and 9. A diurnal cycle consisting of one peak is deemed unimodal, two peaks as bimodal, and zero peaks as neither. MCS rainfall is further classified into continuous afternoon and nighttime rainfall to characterize diurnal cycles without peaks. A diurnal cycle is said to have *continuous afternoon rainfall* if MCS rainfall ±3 hours away from the afternoon maximum is at least 85% of the afternoon maximum value. Similarly, a diurnal cycle is deemed to *have continuous nighttime rainfall* if MCS rainfall at 04Z is at least 75% of MCS rainfall at 21Z. The times 21Z and 04Z are selected as they respectively represent the evening minimum and nighttime maximum for instances of bimodal rainfall observed in the diurnal cycles in Figures 4 and 10. The value of 75% is used over 85% due to the longer nighttime averaging period.

For our seasonal analysis, the wettest and driest months (Apr, Oct, and Jan, Jul respectively) are selected to contrast dry and wet seasons. We opt for representative months in our analysis as the typical three-month seasonal delineation e.g. MAM, JJA, etc. may not fit onto the seasonality of rainfall in the Figure 1 averaging regions.

4. Results

4.1 Seasonality of MCSs

A variety of influences modify Congo Basin precipitation only on a seasonal basis. For example, ascent associated with both the Tropical Easterly Jet (TEJ) and the northern African Easterly Jet (AEJ) increases mid-level convergence, and consequently precipitation, over the northern Congo in boreal summer (Nicholson 2009), and low-level winds north of 6°N are primarily controlled by cyclonic circulation driven by the Saharan heat low in boreal summer (Pokam et al. 2014). Because these phenomena strongly impact only a portion of the Congo, it is important here to assess seasonal precipitation at the regional scale to best capture differences in total and MCS rainfall.

In Figure 2, the total rainfall rate (solid black line), the MCS rainfall rate (solid red line), and the MCS percent contribution toward total rainfall (dotted red line) are averaged over each Congo averaging region (Fig. 1) for every month of the year. In the two boundary regions (Fig. 2a-b), there is only one wet season and one dry season for both total and MCS rainfall. In the northern boundary region box 1 (Fig. 2a), total and MCS rainfall rates are highest in August averaging 7.7 and 6.1 mm day^{-1} respectively and are lowest in Dec-Jan both averaging <1 mm day^{-1}. The boreal winter minimum in box 1 is seasonally opposite to the minimum of the southern boundary region box 4 which occurs in Jun-Jul (Fig. 2b), and both average <1 mm day^{-1}. However, the box 4 maximum in November is not seasonally opposite to the Aug maximum of box 1, and total and MCS rainfall average 6.7 and 5.1 mm day^{-1} respectively at that time.

MCS percent contributions in box 1 (Fig. 2a) and box 4 (Fig. 2b) plateau before MCS rainfall reaches its respective seasonal maximum. MCS percent contribution plateaus in box 1 at near 80% of total rainfall from May-Oct and in box 4 between 70-75% of total rainfall from Sep-Apr. The plateau is reached as average MCS rainfall surpasses approximately 4 mm day^{-1} in both regions. Thereafter, MCS percent contribution in box 1 and box 4 reaches a minimum of <35% as MCS rainfall falls to ~0 mm day^{-1} in the winter seasons.

Similar to the boundary regions, total and MCS rainfall are highest in late summer/boreal autumn and lowest in the solstitial seasons. In the northern equatorial region box 2 (Fig. 2c), total and MCS rainfall are highest in October averaging 7.5 and 6 mm day^{-1} respectively and are lowest in January averaging 1 mm day^{-1}, thus sustaining MCS rainfall even in the driest season. In the southern equatorial region box 3 (Fig. 2d), total and MCS rainfall are highest in November averaging 8 and 6.5 mm day^{-1} respectively and are lowest in July, also averaging 1 mm day^{-1}.

Unlike the two boundary regions, box 2 (Fig. 2c) and box 3 (Fig. 2d) maintain high average MCS percent contributions of 75-80% of total rainfall throughout the year, even during their respective dry seasons. However, average MCS percent contributions in box 3 decrease to 60% of total rainfall during boreal summer while they remain high in box 2 year-round.

In general, MCS rainfall supports the seasonality of total rainfall in the Congo Basin. All regions comprising the Congo Basin experience one wet season from spring to fall and one dry season in winter in the monthly averages for both total and MCS rainfall. This is consistent with the analysis of Cook and Vizy (2022) which showed that a mistaken impression of bimodal seasonality in the Congo Basin arises when averaging regions that span the equator are used. The highest average MCS rainfall occurs in every region in roughly boreal autumn, and the month of maximum MCS rainfall progresses southward from August in box 1, to October in box 2, and to November in boxes 3 and 4. Boxes 1, 2, and 3 average similar maximum seasonal values (6-6.5 mm day^{-1}) while box 4 averages the least (5 mm day^{-1}). MCS rainfall is lowest in either January or July for all four averaging regions depending on the hemisphere. Averaging regions sufficiently capture the seasonality of rainfall and an individual IMERG grid point analysis of seasonality yielded similar results with few zonal differences (not shown).

In the two equatorial regions, the seasonal cycles of both total and MCS rainfall appear to be bimodal with peaks in the equinoctial seasons. However, because total and MCS rainfall rate averages remain high (>3 mm day^{-1}) during the interim solstitial season, the seasonal cycles are better characterized as unimodal with decreased rainfall during the interim solstitial season.

4.2.1 Equinoctial Seasons – Seasonal Cycle

To better highlight inter-seasonal and regional differences, equinoctial months are assessed separately from solstitial months. In Figure 3, average monthly MCS rainfall (mm day^{-1}) and MCS percent contribution are mapped across the Congo Basin for the equinoctial months April (Fig. 3a-b) and

October (Fig. 3c-d). In April (Fig. 3a), a MCS percent contribution maximum of ≥85% develops in the continental interior centered on 21°E along the Congo River. MCS percent contribution remain high at 80% throughout the basin from 5°S to 5°N and along the southern Atlantic coast. MCS percent contribution decreases meridionally but not symmetrically, tapering off to 70% toward 10°S and to 50-60% toward 10°N. MCS rainfall (Fig. 3b) also decreases with latitude and reaches a minimum in northern box 1, coinciding with the MCS percent contribution minimum. However, MCS rainfall maxima are not necessarily located within the MCS percent contribution maximum centered on 21°E (Fig. 3a) but rather are found along the Atlantic coast, in spots along the 6-7°S latitude band, and at the feet of the Rwenzori mountains around 27°E.

In October (Fig. 3c), the distribution of MCS percent contribution values resembles that of April (Fig. 3a). An MCS contribution of 80% of total rainfall is found from 5°S to 5°N, however, the continental interior maximum observed in April does not form and MCS percent contribution are high (≥70%) throughout all of the Congo, including in northern box 1. Higher MCS contribution in box 1 during October is likely supported by the higher MCS rainfall (Fig. 3d) which exceeds 1 mm day^{-1} throughout the basin.

Both equinoctial seasons share an MCS percent contribution of at least 80% between 5°S and 5°N and an area of high MCS rainfall (≥8 mm day^{-1}) along 27°E near the Rwenzori mountains. MCS rainfall is higher and more well-distributed throughout the Congo Basin in October resulting in a decreased meridional gradient of MCS percent contribution from the equatorial region to 10°. A decrease from 1 mm day^{-1} in October to 0 mm day^{-1} in April along 10°N produces a 20% drop in MCS percent contribution (Fig. 3a-b), suggesting MCS percent contribution is sensitive to low MCS rainfall rates. MCS percent contribution shows less sensitivity to higher MCS rainfall rates as exemplified by the large range of MCS rainfall values (3-8 mm day^{-1}) within the April percent contribution maximum. However, MCS percent contribution insensitivity to MCS rainfall may be dependent on location as a 5–8 mm day^{-1} decrease in MCS rainfall along the southern Atlantic coast in box 4 in October only results in a decrease of 10-15% in percent contribution.

4.2.2 Equinoctial Seasons - Diurnal Cycle

Previous TRMM studies find that MCS counts are highest in the afternoon between 15Z and 18Z in both sub-Saharan Africa (Liu et al. 2019) and in the Congo Basin (Jackson et al. 2009). The half-hour resolution in IMERG V06 offers an improvement over the resolution of TRMM and allows us to more accurately resolve the timing of the MCS diurnal cycle.

Figure 4 displays the diurnal cycles of MCS rainfall (solid lines) and MCS percentage contribution to total rainfall (dashed lines) in April and October averaged over the equatorial (Fig. 4a-b) and boundary (Fig. 4c-d) Figure 1 averaging regions. Diurnal cycles begin at 12Z to more easily compare evening, nighttime and morning rainfall. Total rainfall is not plotted due to its high similarity to MCS rainfall. In April (Fig. 4a) and October (Fig. 4b), MCS rainfall in boxes 2 and 3 is highest at 15Z (1600/1700 Local Time (LT)) and lowest at 10Z (1100/1200 LT). Time zones in the Congo split at approximately 20°E into UTC +1 in the west and UTC +2 in the east. The diurnal cycle of MCS rainfall in box 3 is unimodal with continuous nighttime rainfall in both equinoctial seasons. The diurnal cycle of MCS rainfall in box 2 is classified as continuous through the afternoon and nighttime in April and as bimodal in October with a secondary minimum and maximum at 22Z and 04Z, respectively. In both seasons, nighttime and early morning MCS rainfall in box 2 averages about 1 mm day^{-1} higher than in box 3 but MCS percent contributions in both boxes remain similar. The diurnal cycle of MCS percent contribution is comparatively flat, changing by ~10% between 12Z and 07Z.

In the boundary regions, MCS rainfall is also highest between 15Z-16Z and lowest at 10Z in both April (Fig. 4c) and October (Fig. 4d). Here both regions' diurnal cycles are unimodal but nighttime MCS rainfall is lower than in the equatorial regions. MCS percent contribution is seasonally higher by 5-15% in the wetter boundary region, but is similar between regions in the morning and afternoon between 08Z and 18Z. Overall, MCS percent contribution is lower than in the equatorial regions, particularly when either region is dry.

In the equinoctial seasons, the diurnal cycle of MCS rainfall is similar to that of total rainfall with unimodal rainfall throughout the basin except in box 2. MCS percent contribution remains consistent through the afternoon and night despite large changes in MCS rainfall over the diurnal cycle. Nighttime MCS rainfall is lower than afternoon MCS rainfall for all regions and is lowest in box 1. Equatorial regions distinguish themselves from the boundary regions with continuous nighttime MCS rainfall sustained above 3.5 mm day^{-1} and bimodal rainfall in box 2.

In Figure 5, MCS rainfall is mapped across the Congo Basin at key times in the diurnal cycle identified in Figure 4. Here, MCS rainfall in April and October is shown at the 15Z MCS rainfall afternoon maximum (Fig. 5a-b), the 04Z secondary maximum (Fig. 5c-d), and the 10Z diurnal minimum (Fig. 5e-f). At 15Z, MCS rainfall maxima are found on the eastern and western boundaries of the basin in both April (Fig. 5a) and October (Fig. 5b). The maxima (22-28 mm day^{-1}) along the eastern orography in box 3 and in the northern basin along the Atlantic coast are seasonally invariant and occur to the west of elevated terrain. Additional high MCS rainfall (12-26 mm day^{-1}) occurs on a seasonal basis in the southern interior basin and along the southern Atlantic coast in boreal spring and throughout the northern interior basin in boreal fall.

At 04Z (Fig. 5c-d), MCS rainfall maxima (8-18 mm day^{-1}) surround the continental interior of the basin in both equinoctial seasons with larger rainfall rates in the east. MCS rainfall falls below 4 mm day^{-1} where the 15Z maxima occur. There is little difference in the distribution of maxima between April and October although maxima values are larger in October (Fig. 5d).

At the diurnal minimum 10Z (Fig. 5e-f), MCS rainfall is concentrated within the continental interior close to the Congo River in both April (Fig. 5e) and October (Fig. 5f), but similar to 04Z, MCS rainfall maxima values are slightly higher in October.

Figures 5 shows a distinction in the location of afternoon and nighttime MCS rainfall maxima during the equinoctial seasons. Afternoon MCS rainfall maxima occur along the eastern and western boundaries of the basin while nighttime MCS maxima occur closer to the continental interior. Afternoon

MCS rainfall at 15Z shifts meridionally within the interior basin but changes little in magnitude between April and October while nighttime MCS rainfall at 04Z remains stationary but intensifies in October.

In Figure 6, MCS percent contribution is mapped across the Congo in April and October at the afternoon MCS rainfall maximum 15Z (Fig. 6a-b), the secondary maximum 04Z (Fig. 6c-d), and the diurnal minimum 10Z (Fig. 6e-f). While afternoon MCS rainfall maxima in Figure 5 were found only on the eastern and western boundaries of the basin, MCS percent contribution in April (Fig. 6a) exceeds 80% throughout the eastern and central basin with some locations within 5° of the equator exceeding 90% of total rainfall. Moreover, an ≥80% percent contribution occurs wherever MCS rainfall exceeds 4 mm day^{-1} (see Fig. 5a), well below the maximum values observed at this time. In October (Fig. 6b), MCS percent contribution is more homogenous, and again exceeds 80% wherever MCS rainfall exceeds 4 mm day^{-1} (Fig. 5b).

At 04Z, a 90% MCS percentage contribution is found throughout the continental interior and an 80% MCS percentage contribution is found throughout the basin from 8°S to 8°N in both April (Fig. 6c) and October (Fig. 6d). The 90% MCS percent contribution is centered on the northern Congo river in April and additionally along the southern Congo river in October. MCS rainfall exceeds 80% wherever MCS rainfall rates are 2 mm day^{-1} or greater (see Fig. 5c-d).

At 10Z, MCS percentage contribution is lowest throughout the boundary regions and along the eastern and coastal orography (10-60%) in both April (Fig. 6e) and October (Fig. 6d). A 70% MCS percent contribution is maintained in the continental interior within boxes 2 and 3 where MCS rainfall is sustained above 4 mm day^{-1}.

By examining the diurnal cycle of MCS rainfall and percent contribution, we find that the diurnal cycle of equinoctial MCS rainfall is unimodal in boxes 1, 3, and 4, with a peak at 15Z and a minimum at 10Z (Fig. 5). High nighttime rainfall in box 2 results in continuous afternoon and nighttime rainfall in April and bimodal rainfall in October. The 15Z peak is comprised of seasonally invariant MCS rainfall (≥20 mm day^{-1}) that occurs along the eastern and western boundaries of the Congo Basin, primarily to the west of elevated terrain. Additional high MCS rainfall occurs within the interior of the hemisphere for which summer most recently occurred (e.g. the northern basin in October). At 04Z, MCS rainfall maxima shift away from the eastern and western boundaries and toward the continental interior suggesting propagation of MCSs inland. MCS rainfall almost completely accounts for total rainfall in the continental interior at 04Z (≥90%). Because MCS rainfall rates are on average lower at 04Z than during the 15Z afternoon peak, higher MCS percent contribution at 04Z indicate a drastic reduction in non-MCS rainfall at this time.

In order to assess threshold sensitivity and how MCSs may intensify between the 15Z afternoon and 04Z nighttime maxima, we evaluate MCSs at a higher size threshold (LS MCSs) and at a higher rainfall rate threshold (LRR MCSs). Figure 7 shows the percentage of MCS rainfall contributed by LS MCSs (dashed lines) and LRR MCSs (solid lines) over the diurnal cycle for the representative equinoctial months April (Fig. 7a) and October (Fig. 7b). In April (Fig. 7a), the LS MCS percent contribution increases linearly over the diurnal cycle from its minimum at 10Z-13Z (61%-79% of MCS rainfall) to its maximum at 06-07Z (85-92%). This result agrees with the examination of the MCS diurnal cycle by Nesbitt and Zipser (2006) which found that after afternoon genesis, the median area of MCSs increased over the diurnal cycle with a peak at 09Z. This suggests that on average equinoctial MCS rainfall at 04Z is delivered by larger MCSs compared to 15Z as MCSs develop and expand their cloud shield through the night in accordance with the MCS life cycle (Houze 1981, Roca et al. 2017). Regional variations are small, and the equatorial regions maintain a MCS percent contribution 5-10% higher than the boundary regions throughout the diurnal cycle in April. The diurnal cycle of LRR MCSs is more complicated with a minimum at 10Z followed by small maxima at 20Z, 00Z, and 04Z in all four regions. Our results suggest that more intensely raining MCSs are more uniform through the diurnal cycle than larger MCSs in boreal spring.

In October (Fig. 7b), the diurnal cycle of LS MCSs is similar to that of April (Fig. 7a) although regional differences are smaller from 15Z-06Z. In contrast to April, a clear maximum in LRR MCSs emerges at 04Z-05Z in the equatorial regions with an MCS percent contribution nearly 20% higher than at the 15Z maximum. This suggests that on average MCS rainfall at 04Z is delivered by more intensely precipitating MCSs than at 15Z in boreal autumn, but only in the equatorial regions. While Nesbitt and Zipser (2006) found MCS rain rates did not increase over the diurnal cycle, differences may be attributable to their use of the entire TRMM domain (35°S to 35°N) or to differences in the diurnal cycle that cannot be resolved at the TRMM 3-hour temporal resolution. While our results suggest some congruence in the timing of LS and LRR MCSs, particularly in the early and late morning, Mohr and Zipser (1996) found no significant relationship between size and intensity for MCSs. If LSS and LR MCSs do not underlie the 15Z maximum, then it is likely that this peak arises due to an increase in the number of MCSs.

Figure 7 confirms that our results are insensitive to the size threshold. Despite increasing the size threshold by a factor of four, LS MCSs account for 80-92% of MCS rainfall except at the 10Z diurnal minimum when MCS rainfall is low. Equatorial regions are more insensitive to the threshold than boundary regions. Our results may be somewhat sensitive to the rain rate threshold as MCS rainfall at the increased threshold accounts for only 40-60% of MCS rainfall outside of the 10Z diurnal minimum. This difference in MCS percent contribution between the larger size and rain rate thresholds may be due to differences in their respective range of values. For example, 97% of MCSs are larger than 5000 km^2 (Roca et al. 2017) and MCCs easily achieve sizes of 300,000 km^2 (Laing and Fritsch 1993), a magnitude 100 times larger than our size threshold. However, MCS cores observed in IMERG rarely exceed 800 mm day^{-1}, a magntiude about 10 times larger than our rain rate threshold.

4.3.1 Solstitial Seasons – Seasonal Cycle

Here we examine the seasonality and diurnal cycle of MCS rainfall and MCS percent contribution during the representative months for the solstitial seasons. In Figure 8, average monthly MCS rainfall (mm day^{-1}) and MCS percent contribution are shown for the representative solstitial months, January (Fig. 8a-b) and July (Fig. 8c-d). In January (Fig. 8a), MCS percentage contribution exceeds 80% throughout box 3 and in portions of box 2, but rapidly falls under 50% north of 5°N. A maximum of 85-90% develops close to the equator but less coherently than in April (Fig. 3a). The low MCS percent contribution in box 1 is associated with MCS rainfall under 1 mm day^{-1} (Fig. 8b). In contrast to the equinoctial seasons, MCS rainfall maxima in boreal winter are found only in the east: close to the Rwenzori Mountains and in the eastern portion of box 4.

The distribution of MCS percent contribution in boreal summer (Fig. 8c) differs from both the other solstitial season January (Fig. 8a) and the two equinoctial seasons shown in Figure 3. During boreal summer, a ≥85% MCS percent contribution maximum develops in western box 1 to the north of the Cameroon highlands, not near the continental interior. MCS percent contribution falls under 50% throughout box 4 and along the Atlantic coast south of 0°. In July, MCS rainfall (Fig. 8d) is at a maximum in the northwest, aligning with the percent contribution maximum, and decreases along the meridional gradient of MCS percent contribution.

Figure 8 shows that regional differences in MCS percent contribution between the solstitial seasons are greater than those between the equinoctial seasons. While both box 1 and box 4 peak in MCS rainfall in their respective summer season, the summer MCS percent contribution maximum is found close to the equatorial continental interior in boxes 2 and 3 during austral summer and towards the Sahel in box 1 during boreal summer. In contrast to the equinoctial seasons, solstitial MCS rainfall is concentrated on only one of the lateral boundaries of the Congo. Moreover, low MCS rainfall and percent contribution are zonally uniform in box 1 during austral summer but are not zonally uniform in boreal summer. In both boundary regions, MCS rainfall falls to 0 mm day^{-1} at the edge of the Congo rainforest which dips further south in the interior basin (10°S-0°).

4.3.2 Solstitial Seasons - Diurnal Cycle

Figure 9 displays the diurnal cycles of MCS rainfall (solid lines) and MCS percentage contribution to total rainfall (dashed lines) for the solstitial seasons averaged over the equatorial (Fig. 9a-b) and boundary (Fig. 9c-d) Figure 1 averaging regions. In January (Fig. 9a), the diurnal cycle of MCS rainfall in box 3 is unimodal with a peak at 04Z and the MCS rainfall in box 2 is continuous through the afternoon and night with a maximum at 16Z. Box 3 in January is the only instance of higher MCS rainfall occurring at nighttime and not in the afternoon. In July (Fig. 9b), the diurnal cycle in box 2 is bimodal despite its lower nighttime MCS rainfall compared to box 3 in January. MCS percent contribution in box

3 remain below 60% throughout the diurnal cycle, averaging the lowest MCS percent contribution for either equatorial region in any season.

In the boundary regions, MCS rainfall is unimodal in box 4 in January (Fig. 9c) and is continuous throughout the afternoon and night in box 1 in July (Fig. 9d). In their respective dry seasons, both MCS rainfall and percent contribution are extremely low in boxes 1 and 4, averaging <1 mm day^{-1} and 5-30% of total rainfall throughout the diurnal cycle respectively. Box 1 averages higher MCS rainfall through the night in boreal summer than any other Congo region at any point in the year, highlighting the high seasonality north of 5°N which has the lowest nighttime MCS rainfall through the rest of the year. In contrast, the unimodal diurnal cycle with continuous nighttime MCS rainfall is seasonally invariant in box 4 (barring the dry season).

Figure 9 shows that the diurnal cycle of MCS rainfall changes regionally and seasonally in the solstitial seasons, in contrast to the more uniform equinoctial seasons (Fig. 4). However, in all seasons, rainfall in the Congo is MCS percent contribution retains the flat diurnal cycle also observed in the equinoctial seasons, although it is much lower in value when MCS rainfall is low. Regions with low MCS rainfall (0.5 - 1.5 mm day^{-1}) show an MCS percent contribution (35-60%) and regions with near-zero MCS rainfall (<0.5 mm day^{-1}) show the lowest MCS percent contribution (5-30%).

In Figure 10, MCS rainfall is shown at the afternoon MCS rainfall maximum 15Z (Fig. 10a-b), the secondary maximum 04Z (Fig. 10c-d), and the diurnal minimum 10Z (Fig. 10e-f) for the solstitial seasons. At 15Z, MCS rainfall maxima occur near both lateral boundaries of the basin in January (Fig. 10a) and in July (Fig. 10b) despite only appearing on one boundary in the seasonal average (Fig. 8a-b), and are smaller in magnitude compared to the equinoctial seasons (10 to 18 mm day^{-1}). However, MCS rainfall maxima at 04Z occur near only one lateral boundary, specifically, in the east close to the equator near the Rwenzori Mountains in January (Fig. 10c) and in the northwest close to the Cameroon Highlands in boreal summer (Fig. 10d). At 10Z, MCS rainfall resembles the distribution of 04Z minima (Fig. 10e-f) similar to other seasons.

Figure 10 shows, similar to the equinoctial seasons, 15Z maxima occur along both the eastern and western boundaries and 04Z maxima occur near the continental. Boreal summer is an outlier and is the only season with nighttime MCS rainfall maxima that occur mostly outside of the equatorial regions. Because afternoon MCS rainfall far exceeds nighttime rainfall in the equinoctial seasons, the monthly average largely reflects afternoon. In the solstitial seasons, afternoon and nighttime rainfall are of similar magnitudes. This results in MCS rainfall concentrating on one side of the Congo in the monthly average (Fig. 8) wherever both afternoon and nighttime MCS rainfall occur.

In Figure 11, MCS percent contribution in January and July is mapped across the Congo at the afternoon MCS rainfall maximum 15Z (Fig. 11a-b), the secondary maximum 04Z (Fig. 11c-d), and the diurnal minimum 10Z (Fig. 11e-f). At 15Z, MCS rainfall exceeds 80% in both January (Fig. 11a) and July (Fig. 11b) wherever MCS rainfall exceeds 2 mm day^{-1}, a lower threshold than in the equinoctial seasons. MCS percent contribution rapidly fluctuates between 0% and 90% between 3°N and 8°N in January and between 0° and 9°S in boreal summer where MCS rainfall is very low. This suggests that while MCSs are seasonally uncommon during these regions' winters, they are highly important to total rainfall when they impact that region. This is also observed at 04Z in both January (Fig. 11c) and July (Fig. 11d) in the same regions but areas of 90% MCS contribution are augmented. This does not occur as commonly in the equinoctial seasons when MCS rainfall is low (<1 mm day^{-1}), but can be observed at 10Z in April (Fig. 6e). Similar to the equinoctial seasons, MCS percent contribution is high (≥90%) throughout the continental interior. MCS rainfall maxima at 10Z (Fig 11e-f) follow the destruction of maxima at 04Z and again displays rapidly changing MCS percent contribution (0-90%) where MCS rainfall is extremely low.

Figure 12 shows the percentage of MCS rainfall contributed by LS MCSs (dashed lines) and LRR MCSs (solid lines) over the diurnal cycle for the representative solstitial months January (Fig. 12a) and July (Fig. 12b). Due to extremely low MCS rainfall at the higher threshold, box 1 and box 4 are omitted from their respective dry seasons. In January, the MCS percent contribution of LS MCSs is at a maximum at 06Z-07Z (83-91%) and is at a minimum at 12Z-15Z (63-73%), as in the equinoctial seasons. The MCS percent contribution of LRR MCSs is at a maximum at 04Z for boxes 3 and 4 but similar to the equinoctial seasons, it is not regionally homogenous. A minimum occurs at 10Z across regions. Diurnal cycles in July (Fig. 12b) are similar to those in April. However, boreal summer is the only season out of four where LS MCS and LRR MCS percent contribution is highest in a boundary region (box 1).

Figure 12 shows that LS MCSs increase linearly in percentage contribution of MCS rainfall in all seasons. This suggests that the 04Z maximum and nighttime MCS rainfall more broadly are associated with larger MCSs and afternoon MCS rainfall is not, in agreement with prior MCS studies (Nesbitt and Zipser 2003, Roca et al. 2017). MCS rainfall maxima likely occur at 15Z due to an increase in the number of MCSs in all seasons. Moreover, MCS counts double at 15Z compared 04Z (not shown) as afternoon heating of the surface generates new convective cells. The diurnal cycle of LRR MCSs is more regionally and seasonally variable, but some regions seasonally display a 04Z maximum, suggesting that the 04Z maximum in total MCS rainfall is seasonally associated with more intensely precipitating MCSs.

5. Connections Between Convection and Environmental Conditions

An examination of moist static energy (MSE) profiles is used to understand environmental controls on the seasonal and diurnal cycles of MCS rainfall. This analysis distinguishes between the roles of low-level temperature and moisture variations in producing a vertically unstable environment (e.g., Zhang et al. 2016, Zhou and Cook 2020). MSE is defined as the sum of the energy contributed by dry enthalpy, latent heating, and geopotential in an air parcel according to

$$MSE = c_p T + L_v q + gz, \tag{1}$$

where c_p is the specific heat of dry air at constant pressure, T is air temperature, L_v is the latent heat of vaporization for water, q is specific humidity, g is acceleration due to gravity, and z is height from the surface. When MSE decreases with altitude, the environment is convectively unstable, and vice versa. A neutral MSE profile can indicate that convection is operating to mix heat vertically.

Figure 13 displays vertical profiles of MSE and its components averaged over the regions shown in Fig.1 during their respective wet and dry seasons. All profiles begin at 950 hPa to clear the topography and end at 675 hPa since MSE profiles are similar above this level. Results are summarized below:

- Figure 13a shows MSE profiles averaged over the equatorial regions (boxes 2 and 3). Here, the wet and dry seasons are both associated with unstable (negative) MSE profiles below 725 hPa. An examination of other months (not shown) indicates that these regions are convectively unstable throughout the year.
- Figure 13b shows the moisture components of MSE in the equatorial averaging regions. The dashed gray line is the geopotential component, which is the same in all seasons and regions. Seasonal differences in MSE gradients (Fig. 13a) are associated with this component but they are small - slopes during the dry season are steeper than during the wet season, but by less than 20%.
- The temperature component, c_pT, does not vary seasonally box 3 (Fig. 13c). Low-level warming in box 2 during the dry season mitigates the moisture effect of stabilizing the vertical column (Fig. 2b), but it does not dominate.
- Figure 13d shows MSE profiles in the boundary regions (boxes 1 and 4). Both boundary region wet seasons have negative MSE profiles between 900 and 725hPa. In contrast, the dry season in box 1 has a positive MSE profile below 725hPa; the dry season in box 4 has an overall neutral MSE profile.
- Figure 13e shows seasonal moisture profiles in the boundary regions. The seasonal differences in the signs of the MSE profiles in these regions are replicated in the L_vq profiles.
- Small seasonal changes in the temperature profile (17% and 25%, respectively) do not account for the seasonal changes in the MSE profile (Fig. 13f). Similar to box 2, the temperature profile in box 1 is more negative in the dry season, however, this seasonal change is small compared to the change in the moisture profile.

In summary, during the dry seasons in boundary regions (boxes 1 and 4), which average about 0 mm day^{-1} in MCS rainfall, MSE profiles are positive and neutral, indicating large-scale atmospheric conditions that are unfavorable to deep convection. In the equatorial regions (boxes 2 and 3), where MCS rainfall is sustained even in the relatively dry seasons (averaging >1 mm day^{-1}), MSE profiles remain negative throughout the year. In all regions, seasonal differences in MSE profiles are driven by seasonal changes in the moisture component, L_vq.

Figure 14 displays vertical profiles of MSE at 15Z (dark lines) when all regions experience a precipitation maximum, and at 04Z (light lines) when some regions experience a secondary maximum. All profiles are averaged over the representative months when MCS rainfall is present, meaning year-round in the equatorial regions and during the respective wet seasons of the boundary regions. Results are summarized below:

- MSE profiles in the equatorial regions are negative below 725hPa at 15Z (Fig. 14a). At 4Z, MSE slopes are ~70% steeper (more neutral) than at 15Z below 850 hPa, consistent with differences in MCS precipitation.
- This diurnal difference in the MSE slopes is not due to diurnal differences in the moisture component slopes (Fig. 14b), which increase by only about 6%, but rather by a 50% increase in the slope of the temperature component below 850 hPa (Fig. 14c).
- Profiles of MSE and its components in the boundary regions are shown in Figs. 14d-f. The results are similar to the equatorial regions, with temperature differences dominating the diurnal cycle. Slopes are negative from 875 to 725 hPa and neutral below 875 hPa at 15Z. At 4Z, the slope of MSE profiles below 875 hPa is ~ 50% larger, indicating less favorable conditions for convection. This corresponds to lower nighttime MCS rainfall in these regions compared to the equatorial regions.

In summary, the MCS rainfall 15Z maximum is associated with negative MSE profiles between 875 and 725 hPa. Diurnal differences in MSE profiles are driven primarily by diurnal temperature differences.

6. Summary and Conclusions

Prior research has shown that mesoscale convective storms (MCSs) are frequent and intense in the Congo Basin, delivering at least 70% of Congo rainfall (Nesbitt et al. 2005). In this paper, we clarify the importance of MCSs to Congo rainfall through an evaluation of the seasonal, diurnal, and regional variability of climatological MCS rainfall. Using IMERG precipitation estimates, MCS rainfall is identified every half hour for twenty years via size and rainfall criteria and compared with total rainfall. IMERG's high spatial and temporal resolution, cross-dataset climatological adjustments, and validation in other parts of Africa (Dezfuli et al. 2017) provide confidence in its ability to estimate rainfall in a region where precipitation observations have been historically limited (Washington et al. 2013). Assessment at the regional scale is critical to understanding Congo rainfall because precipitation regimes and its seasonal influences are not homogenous across the basin.

Findings on the seasonality of MCS activity in the Congo Basin are summarized as follows:

- The seasonality of MCS rainfall in the Congo Basin follows the seasonality of total rainfall. Both exhibit one wet season and one dry season. The wet season occurs during spring, summer and fall and the dry season occurs during winter (Cook and Vizy 2021).
- Similar to total rainfall, MCS rainfall is at a maximum in late boreal summer and fall for all regions of the Congo. The month of maximum MCS rainfall progresses southward from August at 5°N-10°N, to October at 0°-5°N, and to November at 10°S-0°.
- The percent contribution of MCS rainfall to total rainfall varies seasonally and regionally as detailed below.

In the equinoctial seasons,

- MCS rainfall is highest (≥8 mm day^{-1}) along the Atlantic coast and adjacent to the eastern orography, i.e., the eastern and western boundaries of the Congo Basin. Maxima north of 2°S in boreal autumn and south of 0° in boreal spring, although there is a maximum to the west of the Rwenzori Mountains (3°S - 0°) in both equinoctial seasons.

- MCS percent contribution maxima (80-85%) are uniform in the continental interior within 5° of the equator, and even higher values (85%-90%) develop around the northern Congo River (17°E-25°E) in boreal spring.

In the solstitial seasons,

- In contrast to the equinoctial seasons, MCS rainfall maxima do not occur simultaneously on the eastern and western boundaries of the Congo Basin. A maximum (≥8 mm day^{-1}) occurs in the west adjacent to the Cameroon Highlands in boreal summer and a maximum (≥6 mm day^{-1}) is in the east close to the Rwenzori Mountains in austral summer.
- Similar to the equinoctial seasons, MCS percent contribution maxima (≥80%) are uniform in the continental interior in boreal winter, but they are less homogenous north of the equator. Additional MCS percent contribution maxima (≥80%) occur between 5°N and 10°N in boreal summer.
- Differences in the location of MCS rainfall and MCS percent contribution maxima in the monthly average are attributed to differences in their maxima timing and location within the diurnal cycle.
- MCS rainfall rates and percent contribution are extremely low (~0 mm day^{-1}, <50%) in winter in both hemispheres between 5° and 10° latitude. In boreal winter, the dryness is zonally uniform between 5°N-10°N, tracing the northern edge of the tropical rainforest. In austral winter, the dryness between 10°S-5°S is not zonally uniform. Low MCS and total rainfall rates also trace the southern perimeter of the tropical forest which dips further south in the continental interior.

Findings about the diurnal cycle of MCSs in the Congo are as follows:

- The diurnal cycle of MCS rainfall is the same as that of total rainfall. In the regional averages, the MCS and total precipitation maxima always occur in the afternoon at 15Z during all seasons. The minimum is always in the late morning at 10Z.

- Bimodal diurnal cycling occurs in the northern equatorial region (0°-5°N) during boreal summer and boreal fall. Here, a second maximum occurs at 04Z and a second minimum occurs at 22Z.

In the equinoctial seasons,

- The diurnal cycle of MCS rainfall is unimodal throughout the Congo except in in the northern equatorial region (0°-5°N) during boreal summer and fall.
- Between the equator and (0°-5°N), MCS rainfall falls continuously throughout the afternoon and night (15Z-04Z) in boreal spring and is bimodal in boreal fall.
- MCS percent contribution varies throughout the diurnal cycle. Between 15Z and 08Z, it ranges between 75%-82% of total rainfall close to the equator (5°S-5°N) and falls to 60%-65% at 10Z (precipitation minimum). At 5°-10° latitude in both hemispheres, it ranges from 62%-80% between 15Z and 08Z and falls to 45-50% at 10Z. The minimum occurs at 10Z as nighttime MCSs continue to dissipate and afternoon MCS generation has not yet begun.
- At the 15Z maximum, high MCS rainfall (up to 26 mm day^{-1}) occurs in both equinoctial seasons along the eastern and western boundaries of the basin adjacent to the Cameroon Highlands, Rwenzori Mountains, and equatorial Atlantic coast. Additional high MCS rainfall (12-26 mm day^{-1}) occurs in the southern continental interior (16°E-25°E) and along the southern Atlantic coast in boreal spring and throughout the northern continental interior (13°E-22°E) in boreal fall. An MCS percent contribution of ≥80% occurs wherever the MCS rainfall exceeds 4 mm day^{-1}.
- At 04Z, strong MCS rainfall (8-12 mm day^{-1}) occurs close to the continental interior biased toward the east. Here an MCS percent contribution of ≥80% occurs wherever average MCS rainfall exceeds 2 mm day^{-1}. An MCS percent contribution of ≥90% occurs over the northern Congo River in both equinoctial seasons and additionally over the southern Congo River in boreal fall.

- At the 10Z minimum, MCS rainfall occurs primarily in the continental interior (15°E-25°E) with a percent contribution of ≥70%.

In the solstitial seasons,

- In contrast to the equinoctial seasons, the diurnal cycle of MCS rainfall is not homogenous across regions or seasonally within regions.
- In the summer season in both hemispheres, the diurnal cycle of MCS rainfall is unimodal south of the equator but it is bimodal between 0°-5°N. Between 5°N-10°N it is continuous throughout the afternoon and night.
- During the winter, average MCS rainfall remains near 0 mm day^{-1} through the diurnal cycle beyond 5° of the equator.
- In both seasons, MCS rainfall maxima at 15Z occur along the eastern and western boundaries to the west of high terrain. Maxima in austral summer are lower than in other seasons (14-18 mm day^{-1}) and have the smallest areal extent.
- At 04Z, high MCS rainfall in austral summer (8-12 mm day^{-1}) occurs primarily in the continental interior toward the east, similar to the equinoctial regions. In boreal summer, high MCS rainfall (8-12 mm day^{-1}) does not occur in the continental interior but instead occurs in the northwestern portion of the basin.
- At the 10Z minimum, MCS rainfall occurs in the continental interior with a percent contribution of ≥70%, and also in NW Congo (9°E-25°E), similar to equinoctial seasons.

Results from examining larger MCSs, with an area ≥10,000 km^2 and rain rates exceeding 25 mm day^{-1} are as follows:

- Larger systems follow the seasonality and distribution of the total population of MCSs but there are differences in the diurnal cycle.

- The contribution of larger MCSs to total MCS rainfall increases linearly through the diurnal cycle from a minimum at mid-day (10Z-13Z; 60%-80%) to a maximum in the early morning (06Z-07Z; 83%-92%). Equatorial regions (within 5° of the equator) remain above 80% throughout the diurnal cycle. Percent contributions mostly above 80% indicate that the sensitivity to the choice of the 2000 km^2 size threshold is small.
- The MCS rainfall peak at 04Z has a greater contribution from larger MCSs compared to the afternoon peak at 15Z.

MCSs that deliver intense precipitation, greater than 100 mm day^{-1}, have the following characteristics:

- Intense storms have the same seasonality and distribution as the total MCS population, but there are differences in the diurnal cycle.
- Diurnal cycles differ depending on season and region. However, in regions with a defined maximum, it always occurs at 04Z. The contribution of intense storms to total MCS rainfall ranges from 20%-55% to in the equinoctial seasons, and from 25%-68% in the solstitial seasons. Large decreases in MCS percent contribution (40-80%) indicates some sensitivity to the 25 mm day^{-1} threshold, particularly when MCS rainfall is low.
- Depending on the season and region, the MCS rainfall peak at 04Z has a greater contribution from more intensely raining MCSs than the peak at 15Z.

Connections to the large-scale environment are as follows:

- Seasonal and diurnal MCS rainfall maxima are associated with negative (unstable) MSE profiles in the lower troposphere.
- This large scale instability is driven seasonally by differences in moisture and diurnally by differences in temperature.

- Lower nighttime temperatures that support atmospheric stability are uniform throughout the Congo.
- The moisture levels that largely control atmospheric stability vary more strongly in the boundary regions than in the equatorial regions, and this leads to stronger seasonality of MCS rainfall in the boundary regions.

This analysis shows that MCS activity in the Congo Basin exhibits complex variations on seasonal and diurnal time scale. Further developing our understanding of these systems is vital to advancing our ability to capture these systems in models and predict their behavior on all time scales. This detailed study of MCS activity in the Congo Basin would not have been possible without the existence of the IMERG dataset, and especially its extension from seven to twenty years by the incorporation of TRMM data. Twenty years of observations is minimal for capturing a climatology, and probably inadequate for detecting precipitation trends. Continued and enhanced production of high resolution datasets at the climatological scale is vital to improve our current understanding of Congo Basin rainfall, especially as the climate continues to change through the twenty-first century.

Acknowledgements: Support from NSF Award #26-1016-20 is gratefully acknowledged. The authors acknowledge the Texas Advanced Computing Center (TACC) at The University of Texas at Austin for providing database resources that have contributed to the research results reported within this paper. URL: http://www.tacc.utexas.edu. The Grid Analysis and Display System software (GrADS) developed at COLA/IGES was used for generating select figures. We also thank the reviewers for their insight.

References

Albrecht, Rachel I., Steven J. Goodman, Dennis E. Buechler, Richard J. Blakeslee, and Hugh J. Christian. "Where Are the Lightning Hotspots on Earth?" *Bulletin of the American Meteorological Society* 97, no. 11 (2016): 2051–68. https://doi.org/10.1175/BAMS-D-14-00193.1.

Balas, N., S. E. Nicholson, and D. Klotter. "The Relationship of Rainfall Variability in West Central Africa to Sea-Surface Temperature Fluctuations." *International Journal of Climatology* 27, no. 10 (2007): 1335–49. https://doi.org/10.1002/joc.1456.

Cook, Kerry H., Vizy, Edward K. "Hydrodynamics of Regional and Seasonal Variations in Congo Basin Precipitation" Submitted to *Climate Dynamics* (2022)

Dezfuli, Amin K., Charles M. Ichoku, George J. Huffman, Karen I. Mohr, John S. Selker, Nick van de Giesen, Rebecca Hochreutener, and Frank O. Annor. "Validation of IMERG Precipitation in Africa." *Journal of Hydrometeorology* 18, no. 10 (2017): 2817–25. https://doi.org/10.1175/JHM-D-17-0139.1.

Durkee, Joshua D., Thomas L. Mote, and J. Marshall Shepherd. "The Contribution of Mesoscale Convective Complexes to Rainfall across Subtropical South America." *Journal of Climate* 22, no. 17 (2009): 4590–4605. https://doi.org/10.1175/2009JCLI2858.1.

Dyer, Ellen L. E., Dylan B. A. Jones, Jesse Nusbaumer, Harry Li, Owen Collins, Guido Vettoretti, and David Noone. "Congo Basin Precipitation: Assessing Seasonality, Regional Interactions, and Sources of Moisture: CONGO BASIN: REGIONAL MOISTURE SOURCES." *Journal of Geophysical Research: Atmospheres* 122, no. 13 (2017): 6882–98. https://doi.org/10.1002/2016JD026240.

Hartman, Adam T. "Tracking Mesoscale Convective Systems in Central Equatorial Africa." *International Journal of Climatology* 41, no. 1 (2021): 469–82. https://doi.org/10.1002/joc.6632.

Herrmann, Stefanie M., and Karen I. Mohr. "A Continental-Scale Classification of Rainfall Seasonality Regimes in Africa Based on Gridded Precipitation and Land Surface Temperature Products." *Journal of Applied Meteorology and Climatology* 50, no. 12 (2011): 2504–13. https://doi.org/10.1175/JAMC-D-11-024.1.

Houze, Robert. "Cloud Clusters and Large-Scale Vertical Motions in the Tropics." *Journal of the Meteorological Society of Japan* 60, no. 1 (1981): 396–410.

Huffman, G. J., Bolvin, D. T., Braithwaite, D., Hsu, K., Joyce, R., Kidd, C., et al. (2019). Algorithm Theoretical Basis Document (ATBD) version 06. NASA Global Precipitation Measurement (GPM) Integrated Multi-satellitE Retrievals for GPM (IMERG). NASA
(PDF) Differences in the Diurnal Variation of Precipitation Estimated by Spaceborne Radar, Passive Microwave Radiometer, and IMERG.

Jackson, Brian, Sharon E. Nicholson, and Douglas Klotter. "Mesoscale Convective Systems over Western Equatorial Africa and Their Relationship to Large-Scale Circulation." *Monthly Weather Review* 137, no. 4 (April 1, 2009): 1272–94. https://doi.org/10.1175/2008MWR2525.1.

Laing, Arlene G., and J. Michael Fritsch. "Mesoscale Convective Complexes in Africa." *Monthly Weather Review* 121 (1993): 2254–63.

Laing, Arlene G., J. Michael Fritsch, and Andrew J. Negri. "Contribution of Mesoscale Convective Complexes to Rainfall in Sahelian Africa: Estimates from Geostationary Infrared and Passive Microwave Data." *Journal of Applied Meteorology* 38 (1998): 957–64.

Laing, Arlene G., Richard E. Carbone, and Vincenzo Levizzani. "Cycles and Propagation of Deep Convection over Equatorial Africa." *Monthly Weather Review* 139, no. 9 (2011): 2832–53. https://doi.org/10.1175/2011MWR3500.1.

Laurent, H., N. D'Amato, and T. Lebel. "How Important Is the Contribution of the Mesoscale Convective Complexes to the Sahelian Rainfall?" *Physics and Chemistry of the Earth* 23, no. 5–6 (1998): 629–33.

Leary, Colleen A., and Robert A. Houze. "The Structure and Evolution of Convection in a Tropical Cloud Cluster." *Journal of the Atmospheric Sciences* 36, no. 3 (1979): 437–57. https://doi.org/10.1175/1520-0469(1979)036<0437:TSAEOC>2.0.CO;2.

Liu, Weiran, Kerry H. Cook, and Edward K. Vizy. "The Role of Mesoscale Convective Systems in the Diurnal Cycle of Rainfall and Its Seasonality over Sub-Saharan Northern Africa." *Climate Dynamics* 52, no. 1–2 (2019): 729–45. https://doi.org/10.1007/s00382-018-4162-y.

Maidment, Ross I., Richard P. Allan, and Emily Black. “Recent Observed and Simulated Changes in Precipitation over Africa.” *Geophysical Research Letters* 42, no. 19 (2015): 8155–64. https://doi.org/10.1002/2015GL065765.

Mohr, Karen I., and Edward J. Zipser. “Mesoscale Convective Systems Defined by Their 85-GHz Ice Scattering Signature Size and Intensity Comparison over Tropical Oceans and Continents.” *Monthly Weather Review* 124 (1996): 2417–37.

Nesbitt, Stephen W., and Edward J. Zipser. “The Diurnal Cycle of Rainfall and Convective Intensity According to Three Years of TRMM Measurements.” *Journal of Climate* 16 (2003): 1456–75.

Nesbitt, Stephen W., Robert Cifelli, and Stephen A. Rutledge. “Storm Morphology and Rainfall Characteristics of TRMM Precipitation Features.” *Monthly Weather Review* 134 (2005): 2702–21.

Nicholson, S. E., B. Some, J. McCollum, E. Nelkin, D. Klotter, Y. Berte, B. M. Diallo, et al. “Validation of TRMM and Other Rainfall Estimates with a High-Density Gauge Dataset for West Africa. Part II: Validation of TRMM Rainfall Products.” *Journal of Applied Meteorology* 42 (2003): 1355–68.

Nicholson, Sharon E. “A Revised Picture of the Structure of the ‘Monsoon’ and Land ITCZ over West Africa.” *Climate Dynamics* 32, no. 7–8 (2009): 1155–71. https://doi.org/10.1007/s00382-008-0514-3.

Nicholson, S. E., D. Klotter, A. K. Dezfuli, and L. Zhou. “New Rainfall Datasets for the Congo Basin and Surrounding Regions.” *Journal of Hydrometeorology* 19, no. 8 (2018): 1379–96. https://doi.org/10.1175/JHM-D-18-0015.1.

Petersen, Walter A., and Stephen A. Rutledge. “Regional Variability in Tropical Convection: Observations from TRMM.” *Journal of Climate* 14 (March 2001): 3566–86.

Pokam, Wilfried M., Caroline L. Bain, Robin S. Chadwick, Richard Graham, Denis Jean Sonwa, and Francois Mkankam Kamga. “Identification of Processes Driving Low-Level Westerlies in West Equatorial Africa.” *Journal of Climate* 27, no. 11 (2014): 4245–62. https://doi.org/10.1175/JCLI-D-13-00490.1.

Roca, R., T. Fiolleau, and D. Bouniol. “A Simple Model of the Life Cycle of Mesoscale Convective Systems Cloud Shield in the Tropics.” *Journal of Climate* 30, no. 11 (2017): 4283–98. https://doi.org/10.1175/JCLI-D-16-0556.1.

Tan, Jackson, George J. Huffman, David T. Bolvin, and Eric J. Nelkin. “Diurnal Cycle of IMERG V06 Precipitation.” *Geophysical Research Letters* 46, no. 22 (2019): 13584–92. https://doi.org/10.1029/2019GL085395.

Vemado, Felipe, and Augusto José Pereira Filho. “Convective Rainfall in Lake Victoria Watershed and Adjacent Equatorial Africa.” *Atmospheric and Climate Sciences* 11, no. 03 (2021): 373–97. https://doi.org/10.4236/acs.2021.113022.

Vizy, Edward K., and Kerry H. Cook. “Mesoscale Convective Systems and Nocturnal Rainfall over the West African Sahel: Role of the Inter-Tropical Front.” *Climate Dynamics* 50, no. 1–2 (2018): 587–614. https://doi.org/10.1007/s00382-017-3628-7.

Vizy, Edward K., and Kerry H. Cook. “Understanding the Summertime Diurnal Cycle of Precipitation over Sub-Saharan West Africa: Regions with Daytime Rainfall Peaks in the Absence of Significant Topographic Features.” *Climate Dynamics* 52, no. 5–6 (2019): 2903–22. https://doi.org/10.1007/s00382-018-4315-z.

Washington, Richard, Rachel James, Helen Pearce, Wilfried M. Pokam, and Wilfran Moufouma-Okia. “Congo Basin Rainfall Climatology: Can We Believe the Climate Models?” *Philosophical Transactions of the Royal Society B: Biological Sciences* 368, no. 1625 (2013): 20120296. https://doi.org/10.1098/rstb.2012.0296.

Zhang, Gang, Kerry H. Cook, and Edward K. Vizy. “The Diurnal Cycle of Warm Season Rainfall over West Africa. Part I: Observational Analysis.” *Journal of Climate* 29, no. 23 (2016): 8423–37. https://doi.org/10.1175/JCLI-D-15-0874.1.

Zhao, Siyu, and Kerry H. Cook. “Influence of Walker Circulations on East African Rainfall.” *Climate Dynamics* 56, no. 7–8 (2021): 2127–47. https://doi.org/10.1007/s00382-020-05579-7.

Zipser, E. J. “Use of a Conceptual Model o the Life-Cycle of Mesoscale Convective Systems to Improve Very Short-Range Forecasts.” *Nowcasting* K.A. Browning, Ed., no. Academic Press (1982): 191–204.

Zipser, E. J., Daniel J. Cecil, Chuntao Liu, Stephen W. Nesbitt, and David P. Yorty. "WHERE ARE THE MOST INTENSE THUNDERSTORMS ON EARTH?" *Bulletin of the American Meteorological Society* 87, no. 8 (2006): 1057–72. https://doi.org/10.1175/BAMS-87-8-10

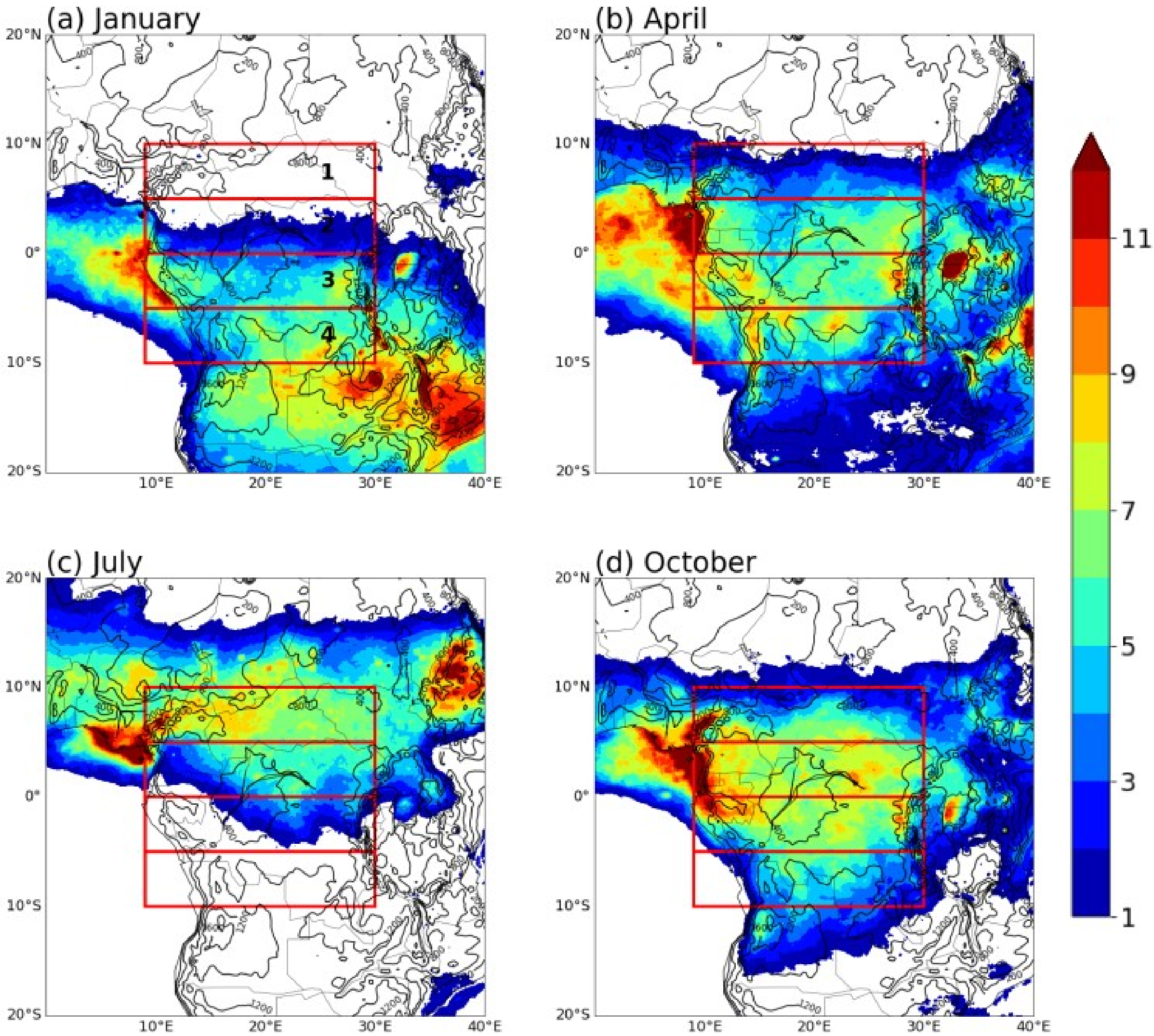

Figure 1. 2001-2020 IMERG climatological precip (mm/day) for (a) January, (b) April, (c) July, and (d) October. Elevation is shown in 400m contour intervals. Location of Congo Basin analysis region (a, red box) and smaller rainfall averaging regions: box 1 (10°N-5°N), box 2 (5°N-0°), box 3 (0°-5°S), and box 4 (5°S-10°S). All averaging regions extend from the Atlantic coast to 30°E.

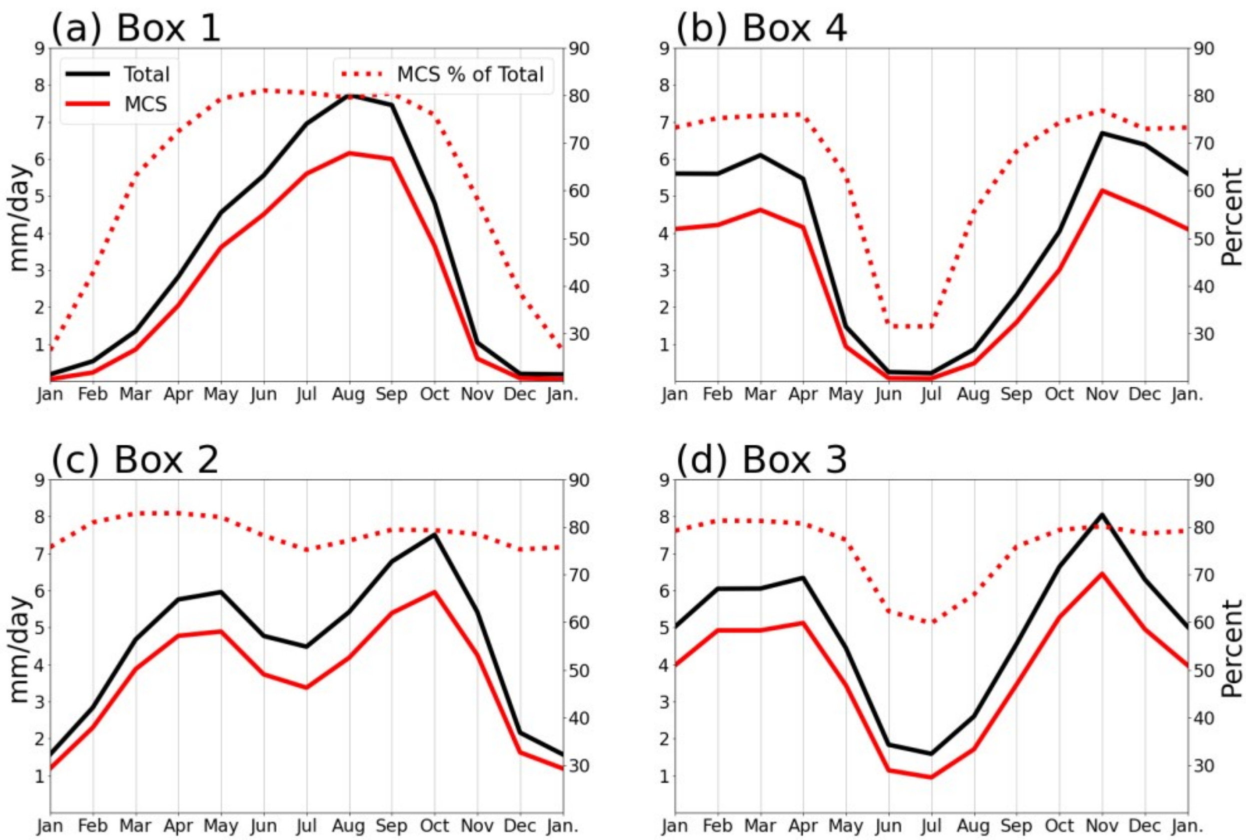

Figure 2. 2000-2020 climatological monthly-mean MCS rainfall (solid red line; mm day^{-1}), total rainfall (solid black line; mm day^{-1}) and percentage of total rainfall delivered by MCSs (dotted red line; percent) averaged over the boundary regions (**a**) box 1 and (**b**) box 4 and the equatorial regions (**c**) box 2 and (**d**) box 3 shown in Figure 1. Rainfall over water is excluded.

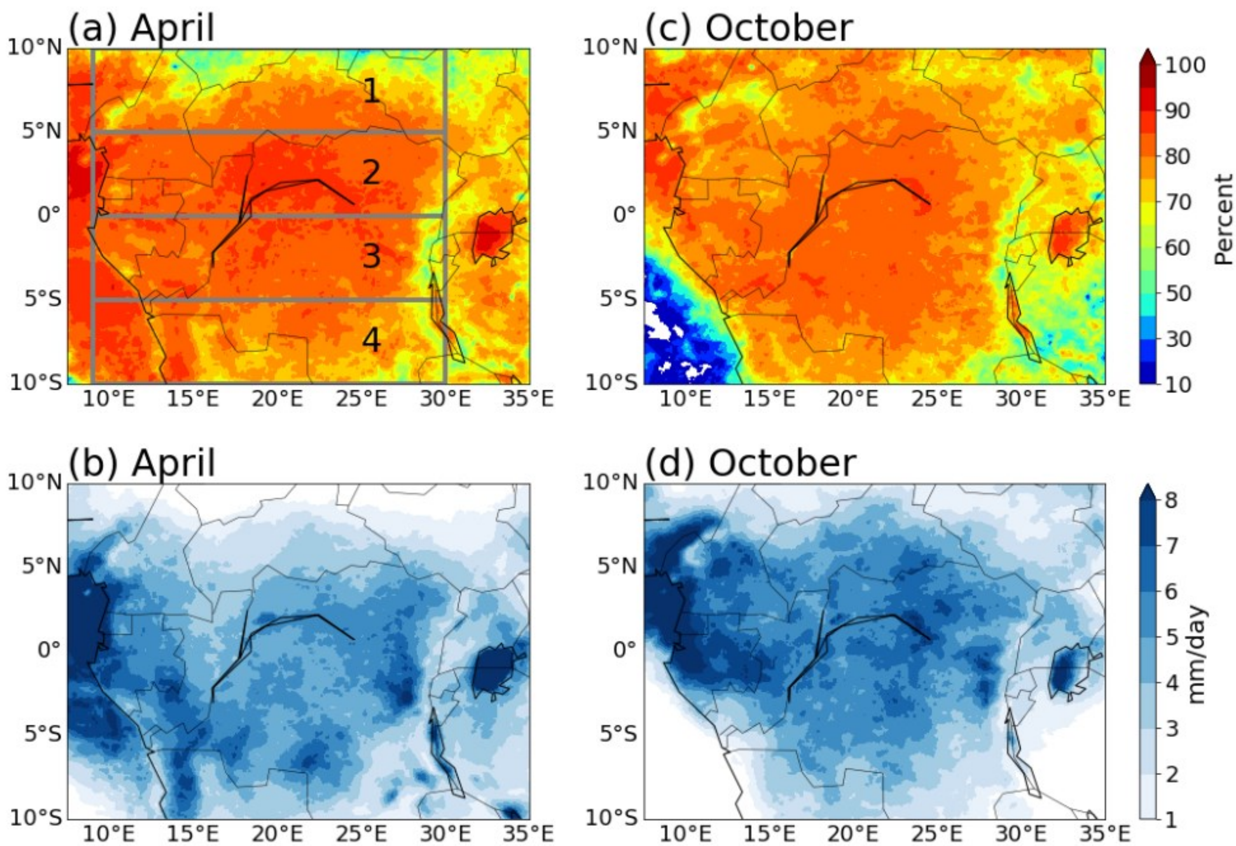

Figure 3. April climatological (**a**) MCS percentage contribution to total rainfall (%) and (**b**) MCS rainfall (mm day^{-1}) at 0.1° resolution. (**c**) and (**d**) are the same as (a) and (b), respectively, but for October.

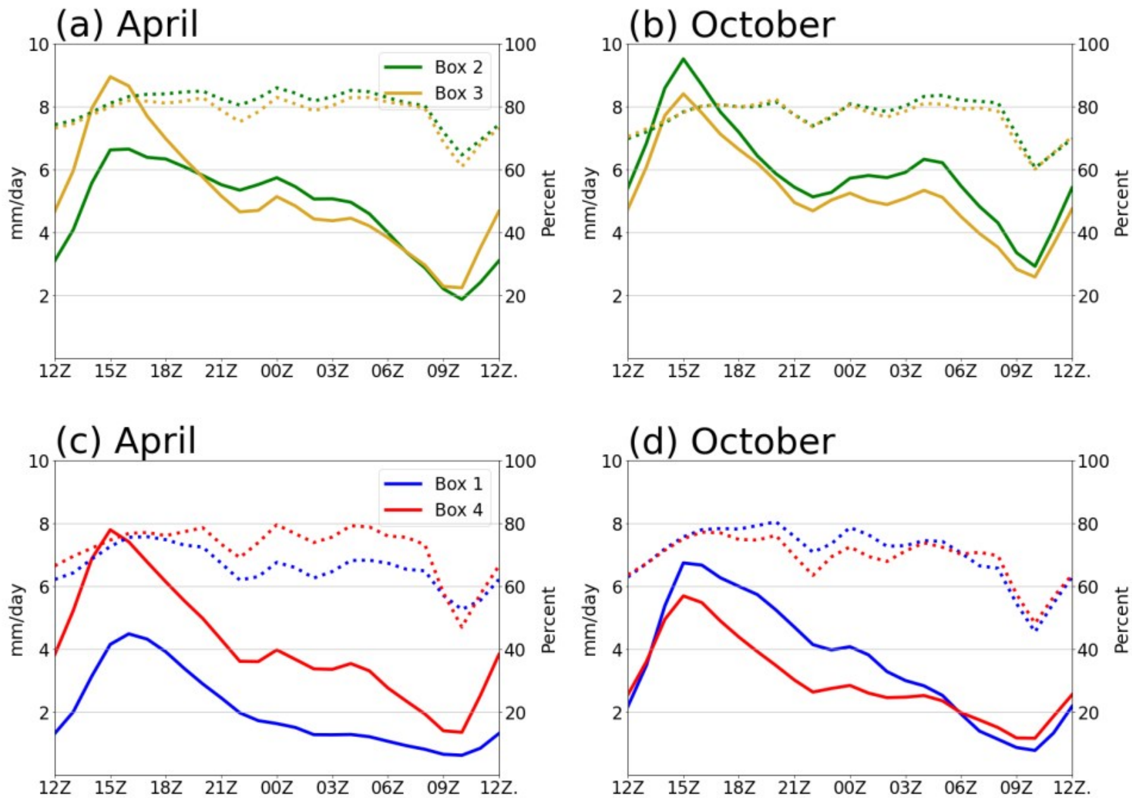

Figure 4. The diurnal cycles of MCS rainfall (solid lines; mm day^{-1}) and MCS percentage contribution (dotted lines, percent) for the box 2 and box 3 averaging regions for (**a**) April and (**b**) October. (**c**)-(**d**) is the same as (a)-(b), respectively, but for box 1 and box 4. Rainfall over water is excluded.

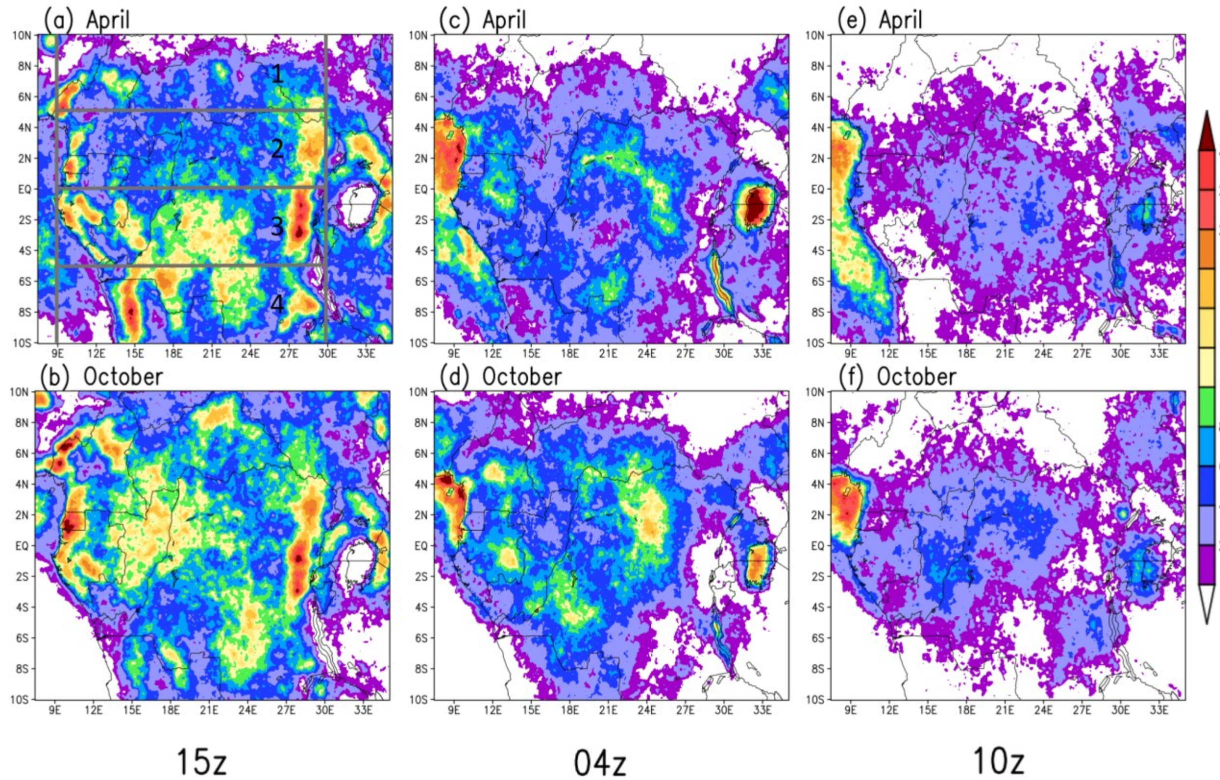

Figure 5. Climatological MCS rainfall (mm day^{-1}) at 0.1° resolution for April and October respectively at (**a, b**) 15Z, (**c, d**) 04Z, and (**e, f**) 10Z.

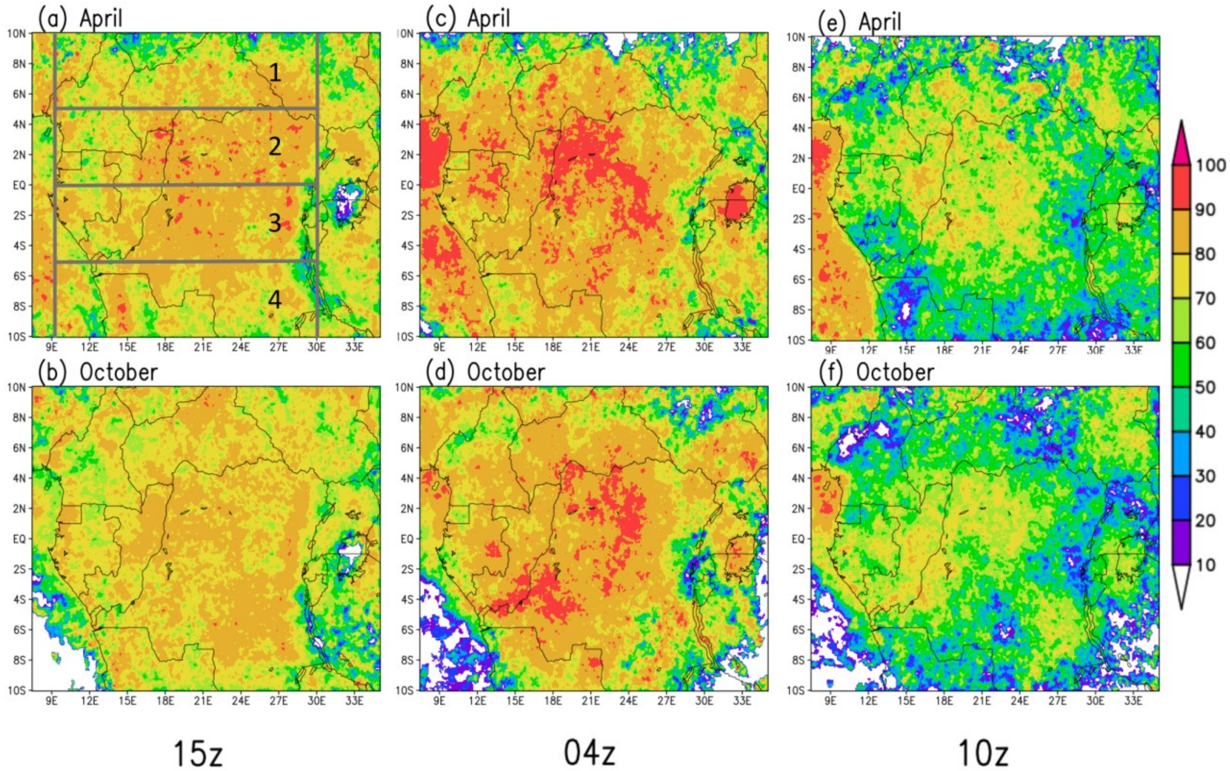

Figure 6. Same as Figure 5, but for MCS percent contribution (%) to total rainfall.

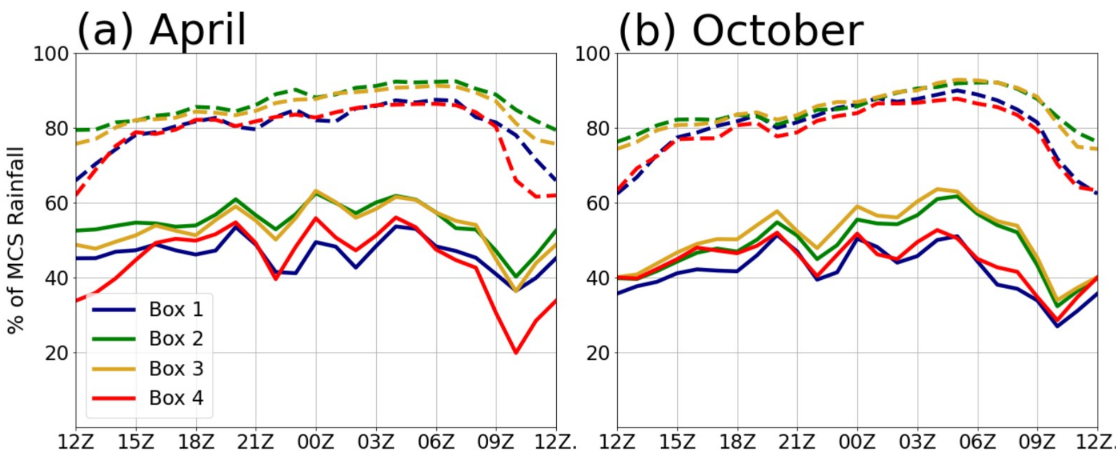

Figure 7. Climatological percentage of MCS rainfall contributed by MCSs at an increased size threshold (dashed lines; 25 mm day^{-1}, 10,000 km^2) and at an increased rain rate threshold (solid lines, 100 mm day^{-1}, 2000 km^2) for Figure 1 averaging regions in (**a**) April and (**b**) October. Percent changes are calculated from the initial MCS criteria: 25 mm day^{-1} and 2000 km^2. Rainfall over water is excluded.

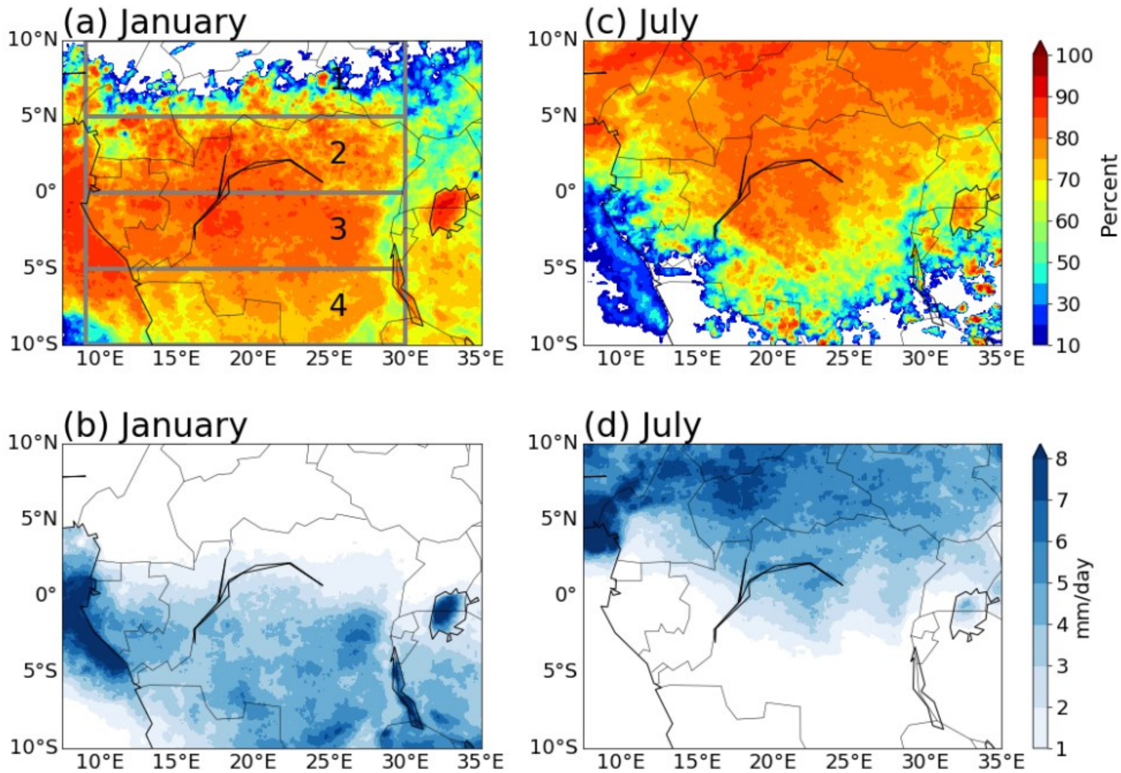

Figure 8. January climatological (**a**) MCS percentage contribution to total rainfall (%) and (**b**) MCS rainfall (mm day^{-1}) at 0.1° resolution. (**c**) and (**d**) are the same as (a) and (b), respectively, but for July.

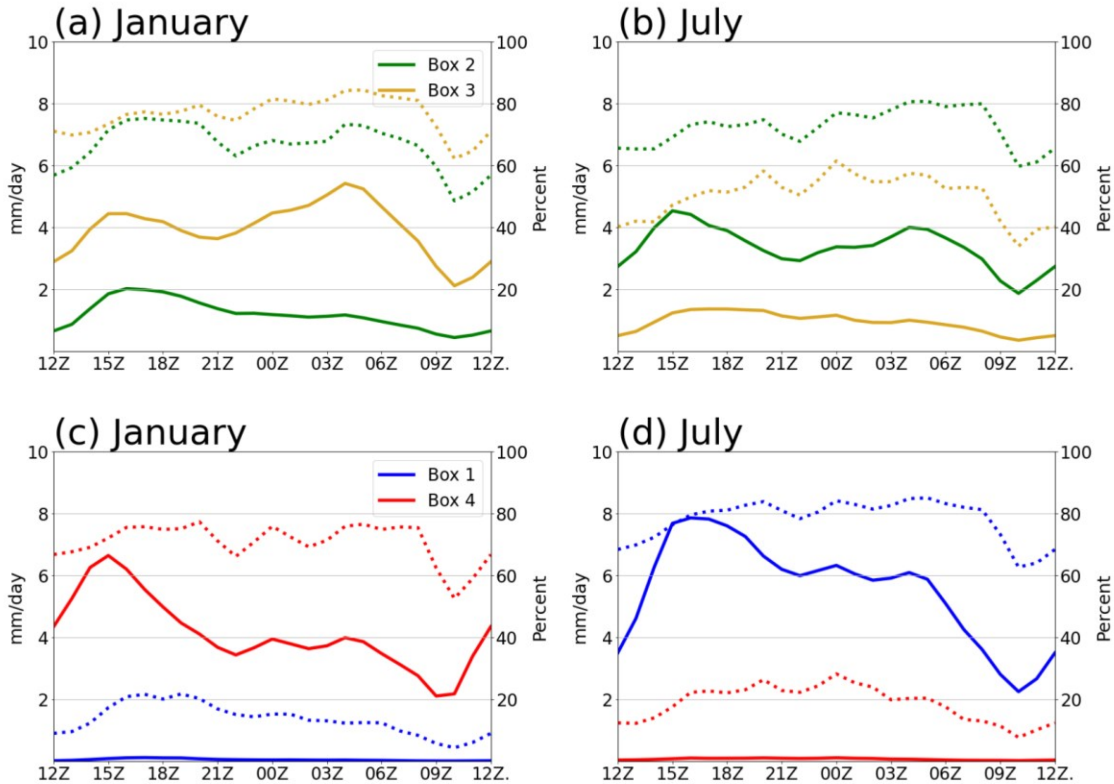

Figure 9. The diurnal cycles of MCS rainfall (solid lines; mm day) and MCS percentage contribution (dotted lines; %) for the box 2 and box 3 averaging regions for (**a**) January and (**b**) July. (**c**) and (**d**) are the same as (a) and (c), respectively, but for box 1 and box 4. Rainfall over water is excluded.

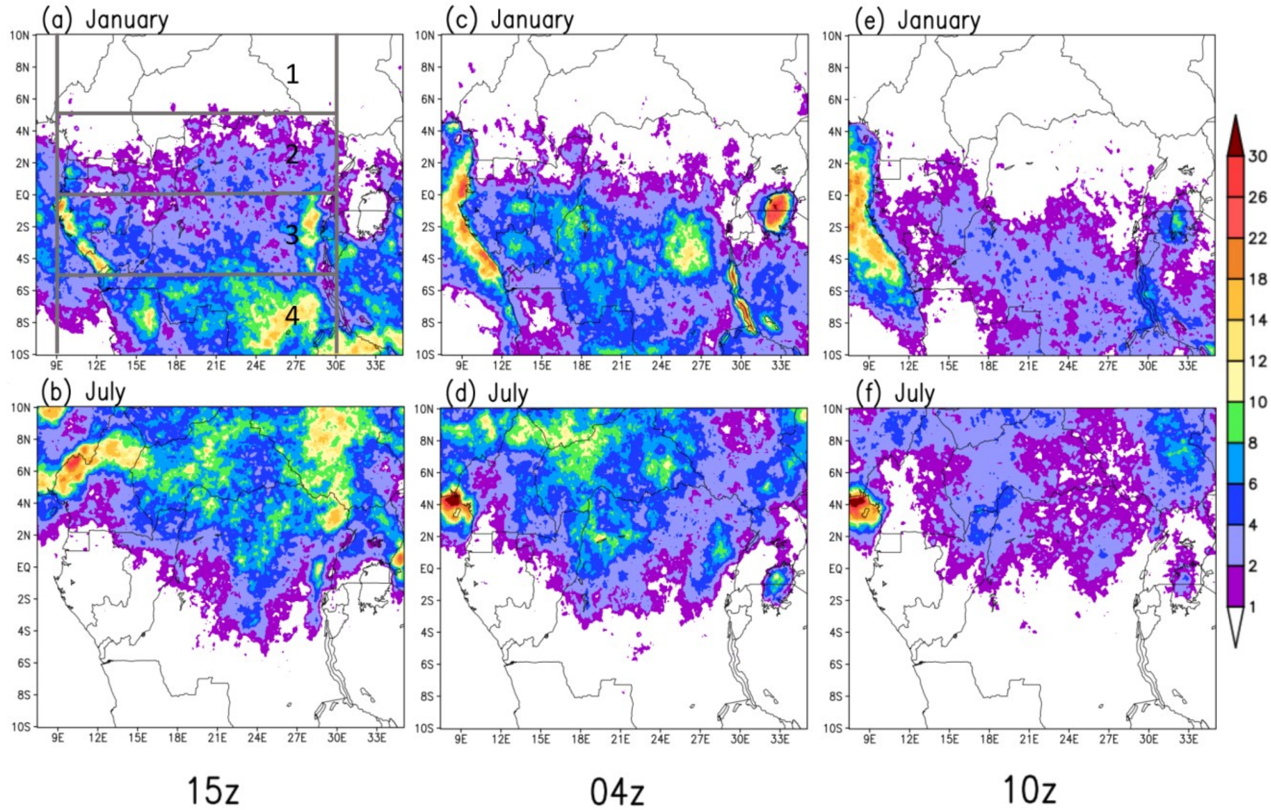

Figure 10. Climatological MCS rainfall (mm day^{-1}) at 0.1° resolution for January and July respectively at (**a, b**) 15Z, (**c, d**) 04Z, and (**e, f**) 10Z.

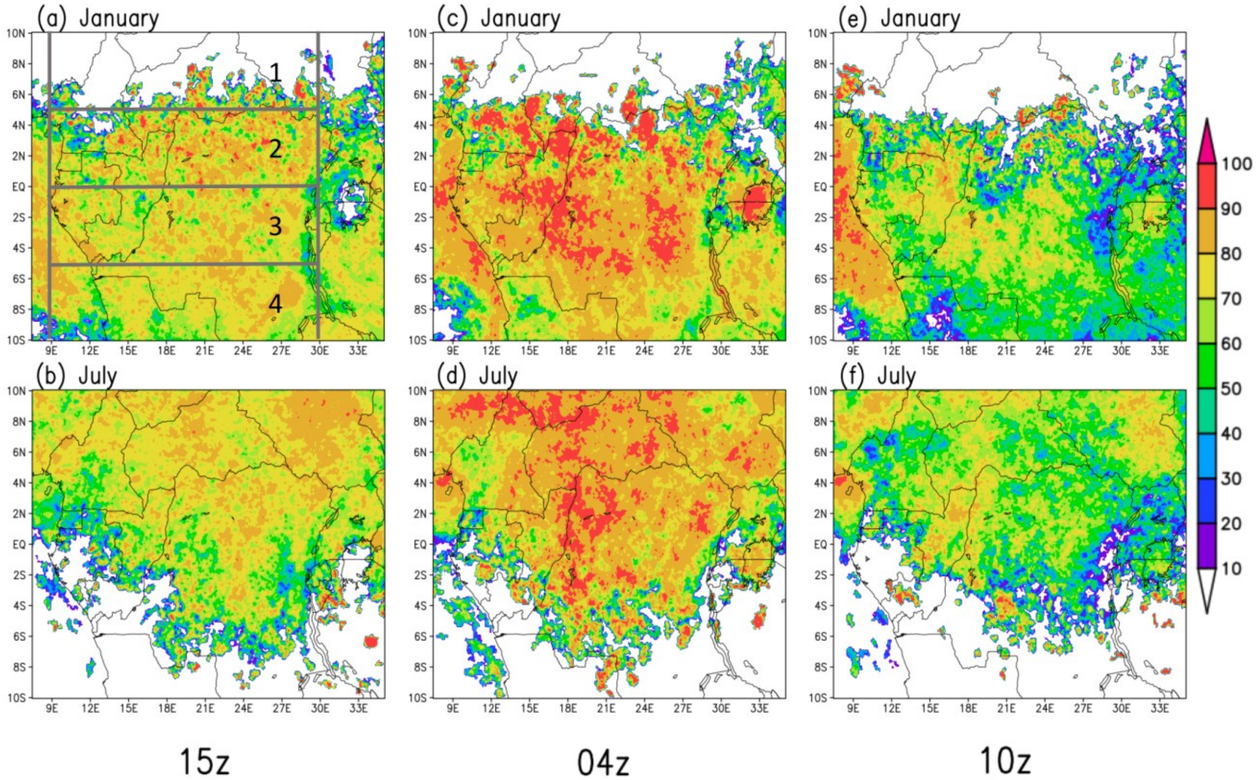

Figure 11. Same as Figure 10, but for MCS percent contribution to total rainfall.

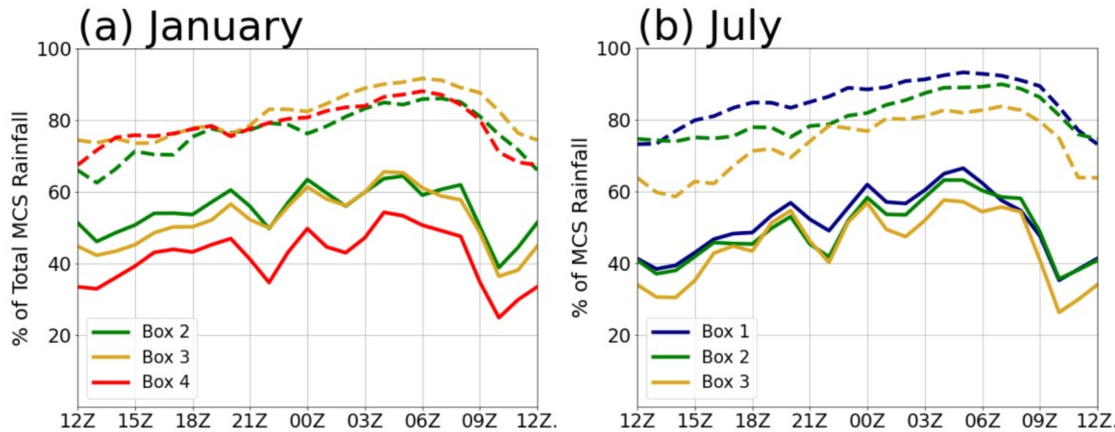

Figure 12. Climatological percentage of MCS rainfall contributed by MCSs at an increased size threshold (dashed lines; 25 mm day^{-1}, 10,000 km^2) and at an increased rain rate threshold (solid lines, 100 mm day^{-1}, 2000 km^2) for Figure 1 averaging regions in (**a**) January and (**b**) July. Percent changes are calculated from the initial MCS criteria: 25 mm day^{-1} and 2000 km^2. Rainfall over water is excluded.

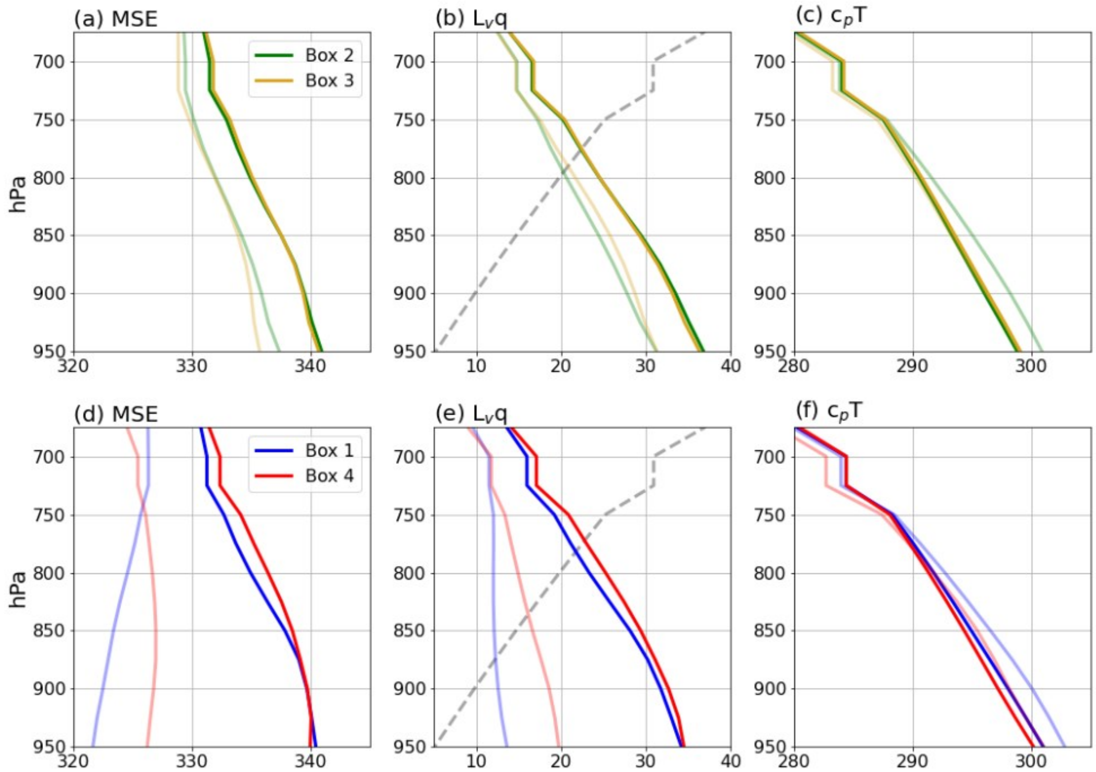

Figure 13. 1979-2020 ERA5 vertical profiles of MSE **(a)**, L_vq **(b)** and c_pT **(c)** averaged over the box 2 and 3 averaging regions for respective wet (dark lines) and dry (light lines) seasons. **(d)** – **(f)** are the same as **(a)** – **(c)** but for boxes 1 and 4. Units are in 10^3 m^2 s^{-2}. Geopotential is included in panel **(b)** and **(e)** (dashed line).

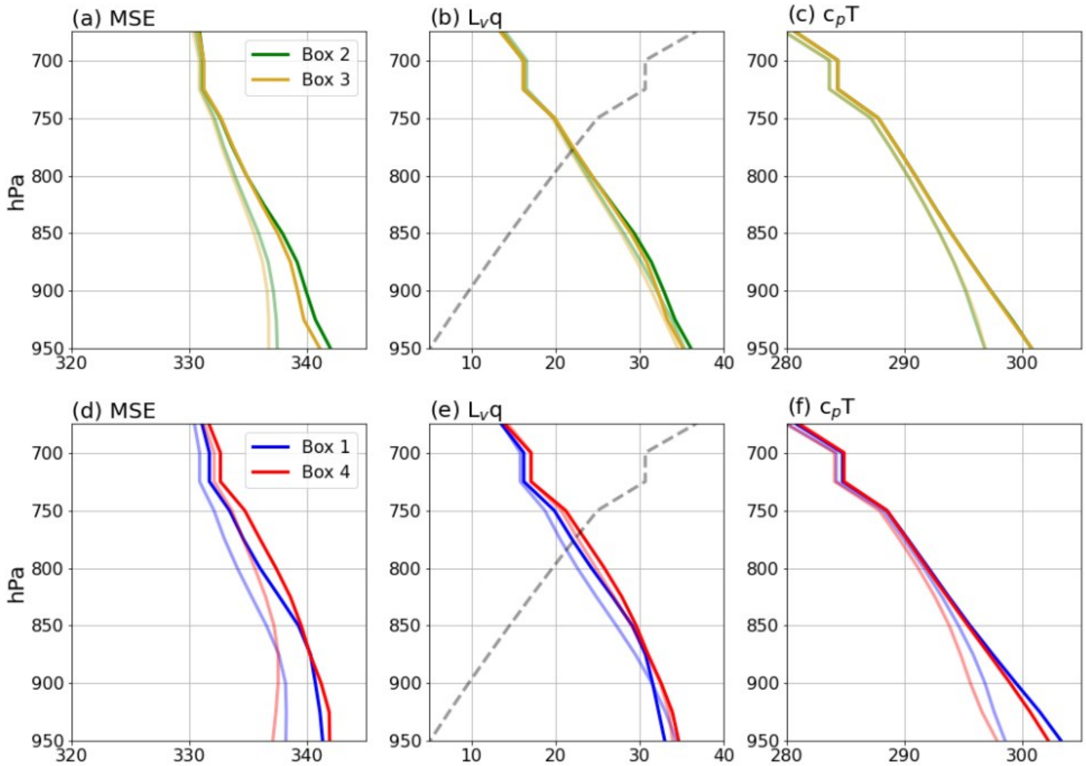

Figure 14. 1979-2020 ERA5 vertical profiles of MSE **(a)**, L_vq **(b)** and c_pT **(c)** averaged over the box 2 and 3 averaging regions at 15Z (dark lines) and 04Z (light lines) for respective wet seasons. **(d)** – **(f)** are the same as **(a)** – **(c)** but for boxes 1 and 4. Units are in 10^3 m^2 s^{-2}. Geopotential is included in panel **(b)** and **(e)** (dashed line).